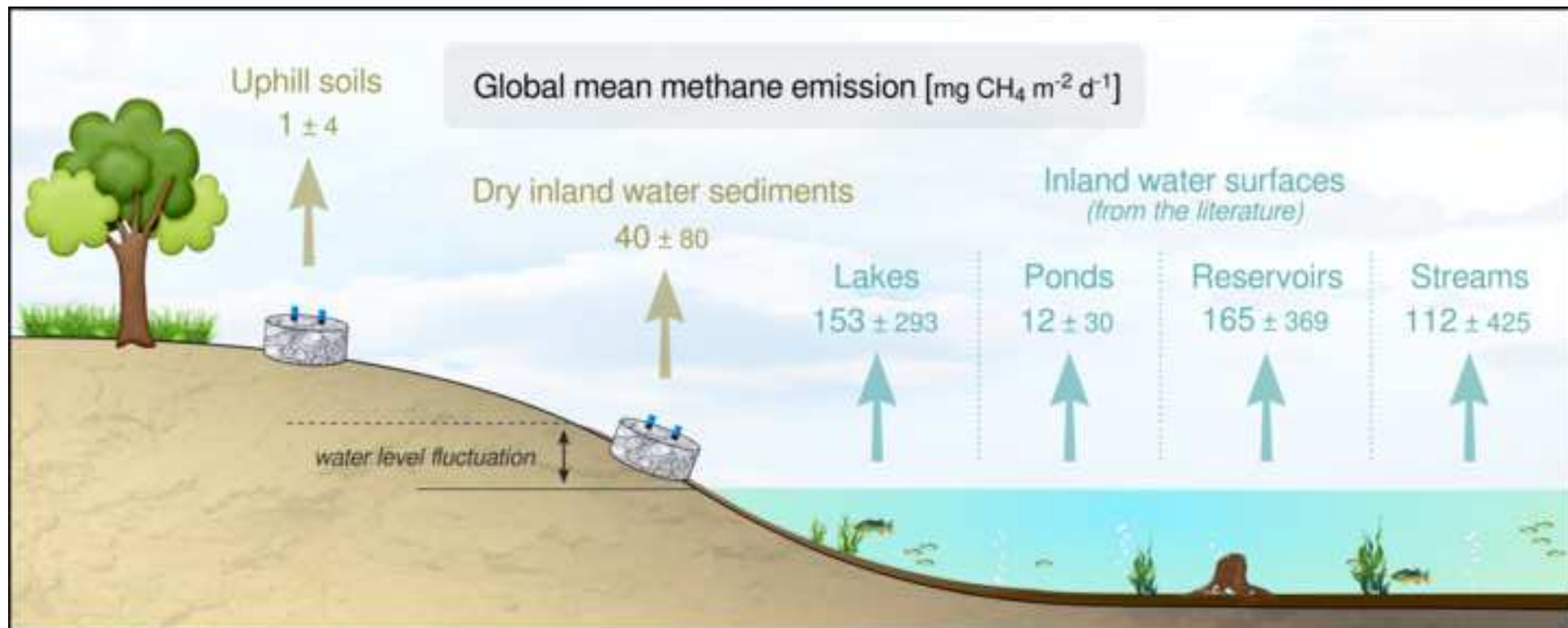


**This is the preprint of the contribution published as:**

Paranaíba, J.R., Aben, R., Barros, N., Quadra, G., Linkhorst, A., Amado, A.M., Brothers, S., Catalán, N., Condon, J., Finlayson, C.M., Grossart, H.-P., Howitt, J., Oliveira Junior, E.S., **Keller, P.S., Koschorreck, M.**, Laas, A., Leigh, C., Marcé, R., Mendonça, R., Muniz, C.C., Obrador, B., Onandia, G., Raymundo, D., Reverey, F., Roland, F., Rõõm, E.-I., Sobek, S., von Schiller, D., Wang, H., Kosten, S. (2022):  
Cross-continental importance of CH<sub>4</sub> emissions from dry inland-waters  
*Sci. Total Environ.* **814** , art. 151925

**The publisher's version is available at:**

<http://dx.doi.org/10.1016/j.scitotenv.2021.151925>



Highlights should be submitted in a separate editable file in the online submission system. Please use 'Highlights' in the file name and include 3 to 5 bullet points (maximum 85 characters, including spaces, per bullet point).

- Dry inland waters are hotspots of C emission to the atmosphere
- CH<sub>4</sub> contributed 10 – 21% to total C emissions (in CO<sub>2</sub>-eq) of dry inland waters
- The contribution of CH<sub>4</sub> (total C emissions) did not differ between types of systems
- Globally, dry inland waters emit 2.7 Tg C-CH<sub>4</sub> y<sup>-1</sup> and emissions are likely rising
- More CH<sub>4</sub> emission data are needed to improve the global GHG budget of inland waters

1 **Cross-continental importance of CH<sub>4</sub> emissions from dry inland-**  
 2 **waters**

3 *José. R. Paranaíba<sup>a,b</sup>✉, Ralf Aben<sup>b</sup>, Nathan Barros<sup>a</sup>, Gabrielle Quadra<sup>a</sup>, Annika*  
 4 *Linkhorst<sup>c,d</sup>, André M. Amado<sup>a,e</sup>, Soren Brothers<sup>f</sup>, Núria Catalán<sup>g</sup>, Jason Condon<sup>h</sup>,*  
 5 *Colin M. Finlayson<sup>i</sup>, Hans-Peter Grossart<sup>j,k</sup>, Julia Howitt<sup>l,†</sup>, Ernandes S. Oliveira*  
 6 *Junior<sup>m</sup>, Philipp S. Keller<sup>n</sup>, Matthias Koschorreck<sup>n</sup>, Alo Laas<sup>o</sup>, Catherine Leigh<sup>p</sup>, Rafael*  
 7 *Marcé<sup>r,s</sup>, Raquel Mendonça<sup>a</sup>, Claumir C. Muniz<sup>m</sup>, Biel Obrador<sup>t</sup>, Gabriela Onandia<sup>u,v</sup>,*  
 8 *Diego Raymundo<sup>x</sup>, Florian Reverey<sup>u</sup>, Fábio Roland<sup>a</sup>, Eva-Ingrid Rõõm<sup>o,w</sup>, Sebastian*  
 9 *Sobek<sup>c</sup>, Daniel von Schiller<sup>t</sup>, Haijun Wang<sup>y</sup>, Sarian Kosten<sup>b</sup>*

10 <sup>a</sup> – Laboratório de Ecologia Aquática, Programa de Pós-Graduação em Biodiversidade e  
 11 Conservação da Natureza, Universidade Federal de Juiz de Fora, Minas Gerais, Brazil.

12 <sup>b</sup> – Department of Aquatic Ecology and Environmental Biology, Radboud Institute for  
 13 Biological and Environmental Sciences, Radboud University, Nijmegen, The  
 14 Netherlands.

15 <sup>c</sup> – Department of Ecology and Genetics, Limnology, Uppsala University, Uppsala,  
 16 Sweden.

17 <sup>d</sup> – Department of Radiology and Monitoring, Federal Institute of Hydrology, Koblenz,  
 18 Germany

19 <sup>e</sup> – Departamento de Oceanografia e Limnologia, Universidade Federal do Rio Grande  
 20 do Norte, Natal, Brazil.

21 <sup>f</sup> – Department of Natural History, Royal Ontario Museum, Toronto, Canada.

22 <sup>g</sup> – Laboratoire des Sciences du Climat et l'Environnement (LSCE), CNRS-UMR 8212,  
 23 France.

24 <sup>h</sup> – Graham Centre for Agricultural Innovation, School of Agricultural & Wine  
 25 Sciences, Charles Sturt University, Wagga Wagga, Australia.

26 <sup>i</sup> – Institute for Land, Water and Society, Charles Sturt University, Albury, Australia.

27 <sup>j</sup> – Department Experimental Limnology, Leibniz Institute of Freshwater Ecology and  
 28 Inland Fisheries, Neuglobsow, Germany.

29 <sup>k</sup> – Institute of Biogeochemistry and Biology, Potsdam University, Potsdam, Germany.

30 <sup>l</sup> – Institute for Land, Water and Society, Charles Sturt University, Wagga Wagga,  
 31 Australia.

32 <sup>m</sup> – Center of Ethnoecology, Limnology and Biodiversity, Laboratory of Ichthyology of  
33 the Pantanal North, University of the State of Mato Grosso, Cáceres, Brazil.

34 <sup>n</sup> – Department of Lake Research, Helmholtz Center for Environmental Research - UFZ,  
35 Magdeburg, Germany.

36 <sup>o</sup> – Institute of Agricultural and Environmental Sciences, Estonian University of Life  
37 Sciences, Tartu, Estonia.

38 <sup>p</sup> – Biosciences and Food Technology Discipline, School of Science, RMIT University,  
39 Bundoora, Victoria 3083, Australia.

40 <sup>r</sup> – Catalan Institute for Water Research (ICRA), Girona, Spain.

41 <sup>s</sup> – Universitat de Girona, Girona, Spain.

42 <sup>t</sup> – Department of Evolutionary Biology, Ecology and Environmental Sciences, Water  
43 Research Institute (IdRA), University of Barcelona, Barcelona, Spain.

44 <sup>u</sup> – Research Platform Data Analysis and Simulation, Leibniz Centre for Agricultural  
45 Landscape Research, Müncheberg, Germany.

46 <sup>v</sup> – Berlin-Brandenburg Institute of Advanced Biodiversity Research (BBIB), Berlin,  
47 Germany

48 <sup>x</sup> – Instituto de Biologia, Universidade Federal de Uberlândia, Uberlândia Brazil.

49 <sup>w</sup> – Environmental Investment Centre, Tallinn, Estonia.

50 <sup>y</sup> – Institute for Ecological Research and Pollution Control of Plateau Lakes, School of  
51 Ecology and Environmental Science, Yunnan University, Kunming, China.

52 † – *In memoriam*

53

54 ✉ Corresponding author:

55 José R. Paranaíba

56 Federal University of Juiz de Fora, Minas Gerais, Brazil

57 Campus Universitário – Rua José Lourenço Kelmer, São Pedro, Juiz de Fora, Minas  
58 Gerais, Brazil. 36036-900

59 e-mail: [jose.paranaiba@ecologia.ufjf.br](mailto:jose.paranaiba@ecologia.ufjf.br)

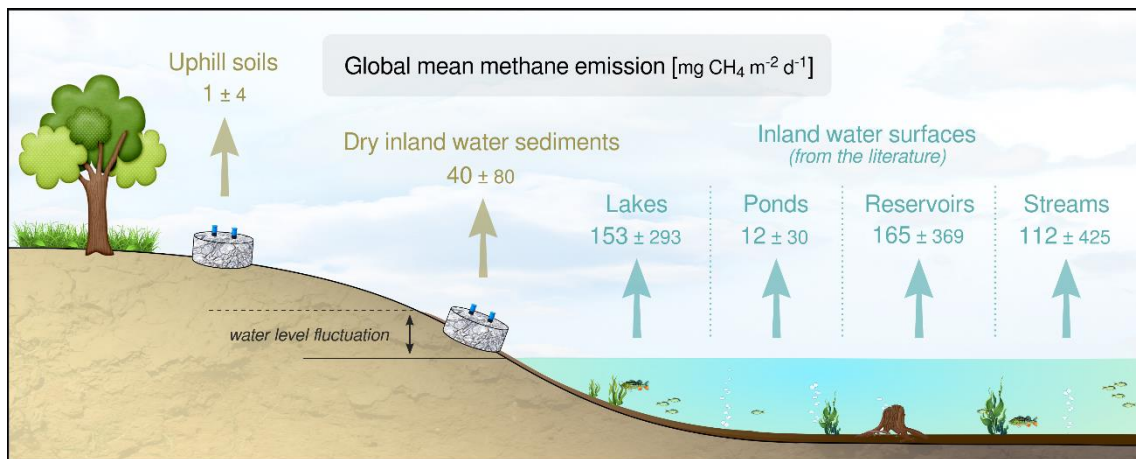
60

61

62

63

64 **Graphical abstract**



65

66

67

68

69

70

71

72

73

74

75

76

77

78

79 **Abstract**

80 Despite substantial advances in quantifying greenhouse gas (GHG) emissions from dry  
81 inland waters, existing estimates mainly consist of carbon dioxide (CO<sub>2</sub>) emissions.  
82 However, methane (CH<sub>4</sub>) may also be relevant due to its higher Global Warming  
83 Potential (GWP). We report CH<sub>4</sub> emissions from dry inland water sediments to i)  
84 provide a cross-continental estimate of such emissions for different types of aquatic  
85 systems (i.e., lakes, ponds, reservoirs, and streams) and climate zones (i.e., tropical,  
86 continental, and temperate); and ii) determine the environmental factors that control  
87 these emissions. CH<sub>4</sub> emissions from dry inland waters were consistently higher than  
88 emissions observed in adjacent uphill soils, across climate zones and in all aquatic  
89 systems except for streams. However, the CH<sub>4</sub> contribution (normalized to CO<sub>2</sub>  
90 equivalents; CO<sub>2</sub>-eq) to the total GHG emissions of dry inland waters was similar for all  
91 types of aquatic systems and varied from 10 – 21%. Although we discuss multiple  
92 controlling factors, dry inland water CH<sub>4</sub> emissions were most strongly related to  
93 sediment organic matter content and moisture. Summing CO<sub>2</sub> and CH<sub>4</sub> emissions  
94 revealed a cross-continental average emission of  $9.6 \pm 17.4$  g CO<sub>2</sub>-eq m<sup>-2</sup> d<sup>-1</sup> from dry  
95 inland waters. We argue that increasing droughts likely expand the worldwide surface  
96 area of atmosphere-exposed aquatic sediments, thereby increasing global dry inland  
97 water CH<sub>4</sub> emissions. Hence, CH<sub>4</sub> cannot be ignored if we want to fully understand the  
98 carbon (C) cycle of dry sediments.

99 **Keywords:** Methane; Dry sediments; Aquatic ecosystems; Greenhouse gases;

100

101

## 102      **1. Introduction**

103            Inland waters (e.g., lakes, ponds, reservoirs, rivers) are complex ecosystems that  
104 process large amounts of allochthonous and autochthonous organic matter (Attermeyer  
105 et al., 2017; Clair and Ehrman, 1996; Friedl and Wüest, 2002; Van Cappellen and  
106 Maavara, 2016) and play important roles as sources and sinks within the global C cycle  
107 (Cole et al., 2007; Rosentreter et al., 2021; Tranvik et al., 2009). In aquatic ecosystems,  
108 organic matter undergoes various biogeochemical processes, including its  
109 decomposition into gaseous carbon (C) species (Mattson and Likens, 1992) such as  
110 carbon dioxide (CO<sub>2</sub>) and methane (CH<sub>4</sub>) (Bastviken et al., 2011; DelSontro et al.,  
111 2018; Raymond et al., 2013). In addition, part of the organic matter can settle and  
112 accumulate in sediments (Heathcote et al., 2015; Mendonça et al., 2017). According to  
113 C-budget studies, approximately 0.06 – 0.25 Pg C y<sup>-1</sup> are estimated to be buried in  
114 sediments of inland waters worldwide (Anderson et al., 2020; Mendonça et al., 2017),  
115 whereas approximately 3.9 Pg C y<sup>-1</sup> are emitted from inland waters to the atmosphere as  
116 CO<sub>2</sub> and as CH<sub>4</sub> (Drake et al., 2018).

117            After CO<sub>2</sub>, CH<sub>4</sub> is the most important gas contributing to the global greenhouse  
118 effect. Considering the Global Warming Potential (GWP) over a 100-year time horizon,  
119 one gram of CH<sub>4</sub> exerts an atmospheric heating power equivalent to 34 grams of CO<sub>2</sub>  
120 (Myhre et al., 2013). Globally, approximately 0.15 Pg of C are annually emitted from  
121 freshwaters to the atmosphere as CH<sub>4</sub> (not considering wetlands, rice paddies and  
122 aquaculture ponds). About 0.13 Pg C y<sup>-1</sup> of these emissions evade to the atmosphere  
123 from lentic (non-flowing) aquatic systems such as lakes, ponds and reservoirs, and  
124 ~0.02 Pg C y<sup>-1</sup> from lotic (flowing) systems such as streams and rivers (Rosentreter et  
125 al., 2021). A large part of the CH<sub>4</sub> production in aquatic systems occurs in anoxic  
126 sediments via microbial degradation of organic matter (Bastviken et al., 2004). The

127 resulting CH<sub>4</sub> that escapes microbial oxidation at the sediment-water interface and water  
128 column (Granéli et al., 1996; Heilman and Carlton, 2001) reaches the atmosphere  
129 through diffusion (Bastviken et al., 2004; Cole and Caraco, 1998), ebullition (bubbling)  
130 (Bastviken et al., 2004), plant-mediated transport (Abril et al., 2005), and by the passage  
131 of deep, CH<sub>4</sub>-rich waters through the turbines of hydroelectric reservoirs (“degassing”)  
132 (Abril et al., 2005; Kemenes et al., 2016). In addition, even after exposure to  
133 atmospheric air, sediment CH<sub>4</sub> production can continue in anoxic microhabitats (Dalal  
134 et al., 2008; Serrano-Silva et al., 2014). However, a large share of the CH<sub>4</sub> produced in  
135 these micro-regions is oxidized to CO<sub>2</sub> by methanotrophic bacteria before evasion to the  
136 atmosphere, especially during the first hours or days after atmospheric exposure  
137 (Koschorreck, 2000). The remaining CH<sub>4</sub> may directly diffuse to the atmosphere.

138         Many inland water ecosystems worldwide experience periods of drying (Marcé  
139 et al., 2019; Messenger et al., 2021). Drying can result from natural (i.e., intermittency of  
140 rivers and ponds) or human-induced (i.e., human actions in reservoirs and lakes) water  
141 level and flow fluctuations (Beaulieu et al., 2018; Di Baldassarre et al., 2018; Leigh et  
142 al., 2016; Wurtsbaugh et al., 2017). During the dry season, considerable areas of  
143 marginal aquatic sediments are exposed directly to the atmosphere. Pekel et al. (2016)  
144 estimated that ~800,000 km<sup>2</sup> (or 18%) of the global surface area that is covered by  
145 inland waters are subject to seasonal atmospheric exposure, especially non-flowing  
146 reaches, which dominate the hydrological networks (Messenger et al., 2021). Moreover,  
147 15% of the global reservoir surfaces are dry (Keller et al., 2021).

148         Exposed aquatic sediments may represent a substantial source of GHG to the  
149 atmosphere (Keller et al., 2020; Marcé et al., 2019; von Schiller et al., 2014) but are  
150 seldom considered in global C emission estimates. Local, regional, and global GHG  
151 emission estimates from dry inland waters have emerged and improved considerably in

152 the last decade (Beaulieu et al., 2018; Gallo et al., 2014; Harrison et al., 2017; Jin et al.,  
153 2016; Marcé et al., 2019), especially for CO<sub>2</sub> (Almeida et al., 2019; Catalán et al., 2014;  
154 Deshmukh et al., 2018; Keller et al., 2020; Obrador et al., 2018; von Schiller et al.,  
155 2014). Keller et al. (2020) found that  $0.12 \pm 0.13$  Pg C y<sup>-1</sup> are added to recent global  
156 inland water C emission estimates when CO<sub>2</sub> emissions from dry inland waters are  
157 considered. However, compared to CO<sub>2</sub>, other GHGs have been poorly assessed in  
158 drying sediments, preventing a complete picture of their role in biogeochemical cycling.  
159 Particularly for CH<sub>4</sub>, the number of studies on dry inland waters is not sufficient to  
160 reliably upscale CH<sub>4</sub> fluxes of these habitats to the global scale (Marcé et al., 2019).  
161 Because of this, a recent global estimate of GHG emissions from dry reservoir  
162 sediments assumed zero CH<sub>4</sub> emissions (Keller et al., 2021). In addition, the  
163 environmental drivers regulating CH<sub>4</sub> fluxes from dry inland waters are not fully  
164 understood. Therefore, the contribution of CH<sub>4</sub> emission from exposed sediments to  
165 global C emission from inland waters remains to be quantified.

166         This study aims to assess the importance of CH<sub>4</sub> fluxes from the exposed  
167 sediments of different types of aquatic systems (i.e., lakes, ponds, reservoirs, and  
168 streams) located in various climate zones across the globe. To achieve this, dry inland  
169 water CH<sub>4</sub> fluxes were i) compared to CH<sub>4</sub> fluxes observed in adjacent uphill (natural  
170 terrestrial) soils; ii) compared to the CO<sub>2</sub> fluxes obtained at the same locations where  
171 CH<sub>4</sub> fluxes were measured; iii) related to physical and chemical sediment properties that  
172 were concurrently measured along with CH<sub>4</sub> in order to identify drivers of CH<sub>4</sub> fluxes  
173 from exposed sediments; iv) scaled up to the respective dry global surface areas  
174 associated with each type of aquatic system studied here, to v) ultimately determine  
175 whether dry inland water CH<sub>4</sub> fluxes represent a significant share of the global C  
176 emission estimates from inland waters. To the best of our knowledge, this is the first

177 cross-continental study quantifying the magnitude and environmental controls of CH<sub>4</sub>  
178 fluxes from the dry sediments of multiple aquatic system types.

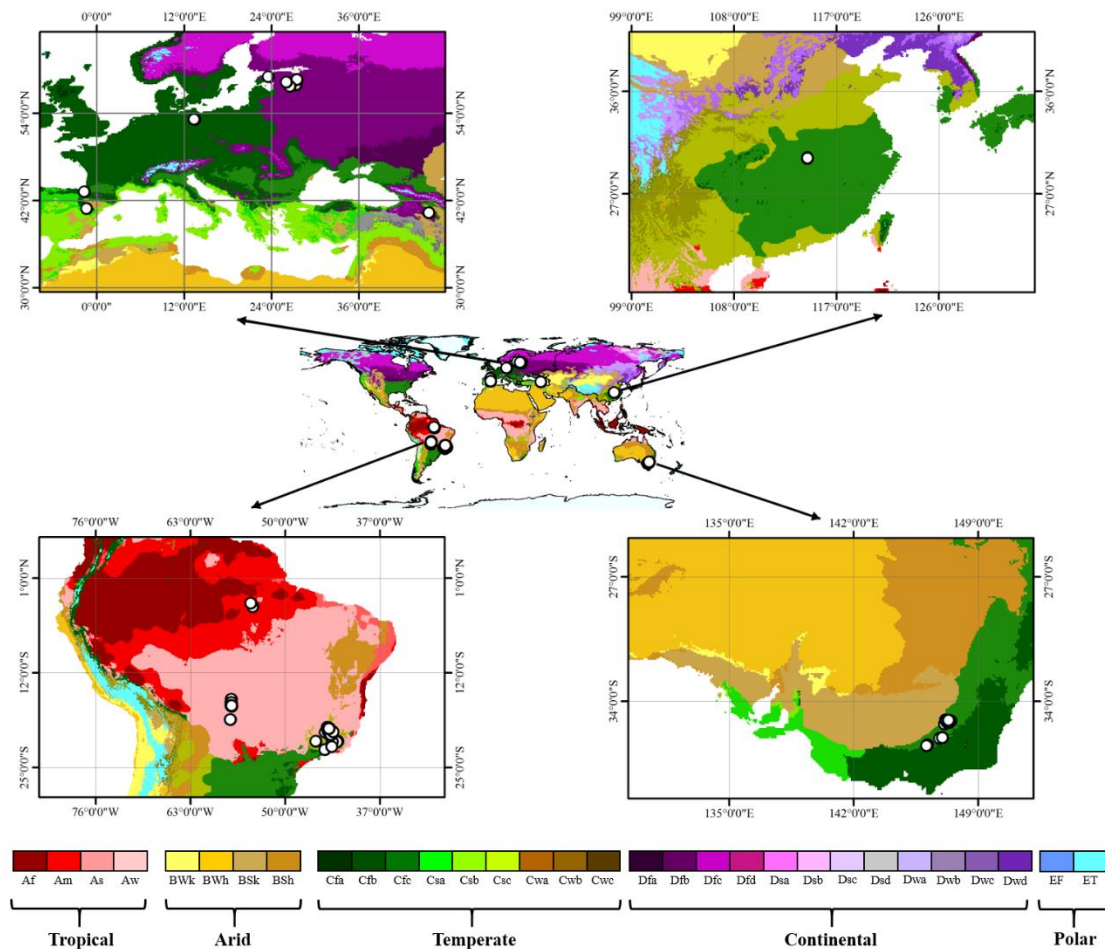
179

## 180 2. Methods

### 181 2.1 Studied sites and sampling strategy

182 This study includes measurements in 89 hydrologically independent aquatic  
183 systems (lakes,  $n = 45$ ; ponds,  $n = 16$ ; reservoirs,  $n = 19$ ; and streams,  $n = 9$ ), located in  
184 three of the five global climate zones (tropical,  $n = 24$ ; continental,  $n = 11$ ; and  
185 temperate,  $n = 54$ ) (Kottek et al., 2006) (Figure 1), which were conducted by 22  
186 research groups from 10 countries. The research groups were classified as levels of a  
187 variable named “*research group*”, which were used in the analysis of CH<sub>4</sub> flux drivers  
188 (see below). The 89 systems are a subset of the 196 aquatic systems included in a recent  
189 global study on CO<sub>2</sub> emission from exposed sediments by Keller et al. (2020). The  
190 subset was created based on the availability of CH<sub>4</sub> flux data (i.e., not all datasets  
191 contained CH<sub>4</sub> data).

192 At each sampling site, two distinct regions were sampled: i) exposed sediment –  
193 hereafter named as “*dry inland water*”, which corresponds to an area with air-exposed  
194 sediment that experiences periodic and/or recent historical inundation (Marcé et al.,  
195 2019); and ii) adjacent uphill soil, which corresponds to the adjacent terrestrial region  
196 that is not inundated. At each region, measurements were performed in triplicates that  
197 were, if possible, conducted at least 1 meter apart from each other to capture spatial  
198 within-region variability.



199

200 **Figure 1** | Cross-continental distribution of the sampling sites (white dots) across the  
 201 different climate zones according to the Köppen-Geiger climate classification system  
 202 (Kottek et al., 2006).

203

## 204 **2.2 CH<sub>4</sub> flux measurements**

205 Between 2016 and 2017, *in situ* measurements of CH<sub>4</sub> flux (mg CH<sub>4</sub> m<sup>-2</sup> d<sup>-1</sup>)  
 206 were conducted using opaque chambers connected to infrared gas analyzers in closed  
 207 gas loops. The chambers were gently placed over the sediment/soil surface to avoid  
 208 disturbance and gas leakage during the measurements, and where necessary, sealed with  
 209 clay (Lesmeister and Koschorreck, 2017). Changes in CH<sub>4</sub> partial pressure (*m*CH<sub>4</sub>) were

210 monitored within the chambers over 3-5 minutes, and the fluxes were calculated  
211 following:

$$212 \quad FCH_4 = \left( \frac{dmCH_4}{dt} \right) \times \left( \frac{V}{RTA} \right) \quad (1)$$

213 where  $dmCH_4$  is the slope of change in  $mCH_4$  (ppm) over time ( $dt$ , given in seconds),  $V$   
214 is the volume of the chamber ( $m^3$ ),  $R$  is the gas constant =  $8.205746 \times 10^{-5} m^3 atm mol^{-1}$   
215  $K^{-1}$ ,  $T$  is the air temperature (K), and  $A$  is the surface area covered by the chamber ( $m^2$ ).

216 Dry inland waters lack  $CH_4$  ebullition as an emission route (Marcé et al., 2019),  
217 mainly due to the absence of water overlying the sediments. Therefore, our  
218 measurements represent only the diffusion of  $CH_4$  at the sediment/soil-atmosphere  
219 interface. Opaque chambers were used in order to minimize temperature changes during  
220 measurements, which may affect the gas exchange at the interface between  
221 sediment/soil and headspace (Welles et al., 2001). Chamber deployments were  
222 performed on top of bare sediment/soil, avoiding vegetated surfaces.

223

### 224 **2.3 Sediment/soil characterization**

225 After the flux measurements, surface sediment/soil samples were collected from  
226 the plot of the flux measurement, placed in plastic bags and stored in thermal cooler  
227 boxes for subsequent laboratory analysis. Air and sediment/soil temperature ( $^{\circ}C$ ) were  
228 measured *in situ*, and elevation (m.a.s.l., meters above sea level) was either measured *in*  
229 *situ* or read from a map. Sediment/soil texture was determined following a manipulative  
230 test developed by the Food and Agriculture Organization of the United Nations (FAO,  
231 2020) and distinguished as clay, light clay, heavy loam, sandy loam, loamy sand, and  
232 sand. 10 g of fresh sediment/soil were mixed in 25 mL distilled water for the

233 determination of electrical conductivity ( $\mu\text{S cm}^{-1}$ ) and pH by measuring the suspended  
234 solution (after 1 h standing) with conventional electrodes (Keller et al., 2020). Moisture  
235 content (% weight loss) was determined by drying 5 g of fresh sediment/soil at 105 °C  
236 until reaching a constant weight (Keller et al., 2020). Afterward, the samples were  
237 combusted at 500 °C until constant weight for the determination of the organic matter  
238 content (% weight loss) (Dean, 1974).

239

#### 240 ***2.4 Data analysis and statistical procedures***

241 Each sampling site was assigned to a climate zone according to “The World  
242 Maps of Köppen-Geiger Climate Classification” (Kottek et al., 2006). For each  
243 sampling site, we then calculated the contribution of dry inland water CH<sub>4</sub> emission to  
244 the total (i.e., CO<sub>2</sub> + CH<sub>4</sub>) GHG emission in CO<sub>2</sub>-equivalents (CO<sub>2</sub>-eq; see below how  
245 CH<sub>4</sub> was converted to CO<sub>2</sub>-eq) for each type of aquatic system (lakes, ponds, reservoirs,  
246 and streams). The CO<sub>2</sub> flux data was retrieved from Keller et al. (2020), and each CO<sub>2</sub>  
247 flux measurement was associated with the CH<sub>4</sub> flux measurement collected at the same  
248 sampling site. For all analyses, triplicate measurements were averaged, and one average  
249 value per parameter at each sampling site was used.

250 To test the relationships between environmental variables and dry inland water  
251 CH<sub>4</sub> fluxes, a generalized linear mixed model (GLMM) was performed using the  
252 “*glmer*” function in the “*lme4*” package (Bates et al., 2015) in R (v. 4.0.2) (R Core  
253 Team, 2018). We used sediment texture, sediment temperature, pH, electrical  
254 conductivity, moisture and organic matter content, as well as latitude, elevation, annual  
255 mean precipitation, and annual mean air temperature as fixed effects. Given that CH<sub>4</sub>  
256 fluxes are primarily driven by the availability and quality of organic matter, moisture,

257 and temperature (Aben et al., 2017; Grasset et al., 2018; Koschorreck, 2000; Sobek et  
258 al., 2012; Yvon-Durocher et al., 2014), the interactions between i) organic matter  
259 content and temperature, ii) organic matter and moisture content, and iii) moisture  
260 content and temperature of the sediments were also included as fixed effects. The  
261 variables research group, type of aquatic system, and climate zone were used as crossed  
262 random factors to account for the dependencies in the data. We used GLMM because  
263 preliminary analyses showed that the distribution of the residuals of the linear mixed  
264 models followed a logarithmic distribution and, therefore, the Gamma family (*link=log*)  
265 was applied in the GLMM (Lo and Andrews, 2015). A value of  $13 \text{ mg m}^{-2} \text{ d}^{-1}$  was  
266 added to the  $\text{CH}_4$  flux data (i.e.,  $x + 13$ ) to avoid negative values which would hamper  
267 our GLMM analysis since the Gamma family (*link=log*) does not allow negative values  
268 in the response variable. The observed negative  $\text{CH}_4$  flux values (i.e., influx; see section  
269 3. Results and Discussion) were very small in magnitude compared with emissions –  
270 most of the influx data were close to zero and the strongest influx was roughly  $7 \text{ mg}$   
271  $\text{CH}_4 \text{ m}^{-2} \text{ d}^{-1}$ , whereas the efflux rates were often two orders of magnitude greater than  
272 influx rates. Therefore, the addition of the fixed value aforementioned does not have a  
273 relevant impact on the overall driver analysis. Logarithmic and cubic root  
274 transformations were adopted for electrical conductivity and organic matter content ( $x +$   
275  $1$ ), moisture, and elevation, respectively, to meet the conditions of normality and  
276 homoscedasticity of variances. Before analysis, collinearity between predictor variables  
277 was assessed using the variance inflation factor (VIF) function in the “*usdm*” package  
278 (Naimi et al., 2014) in R. Variables with VIF values  $> 5$  (which is indicative of  
279 collinearity) were excluded from the procedures (Akinwande et al., 2015). In the  
280 GLMM presented here, the excluded variable was annual precipitation. The model was  
281 simplified by removing non-significant predictors. GLMMs were also used to assess

282 differences in CH<sub>4</sub> fluxes, moisture, and organic matter content among aquatic system  
283 types (fixed factor), between sampling regions (fixed factor), and between climate zones  
284 (fixed factor), with the variable research group defined as a crossed random factor.  
285 Type-III ANOVAs were used to test the significance of the fixed factors, with degrees  
286 of freedom and *p* values calculated using the Kenward-Roger approximation (Kenward  
287 and Roger, 1997) through the “*lmerTest*” and “*pbkrtest*” packages (Halekoh and  
288 Højsgaard, 2014; Kuznetsova et al., 2017). Least-square means (classical Yates  
289 contrasts), as well as pairwise differences, were computed by the “*ls\_means*” function  
290 (“*lmerTest*” package). For all statistical procedures, a *p* value < 0.05 was adopted as the  
291 threshold level of statistical significance.

292       Finally, to obtain an estimate of cross-continental CH<sub>4</sub> emission from dry inland  
293 waters, we multiplied the average CH<sub>4</sub> flux rate of each type of aquatic system by its  
294 respective global associated desiccated surface area (for lakes, reservoirs, and ponds:  
295 Marcé et al., 2019; for streams: Raymond et al., 2013), and then summed them up. Also,  
296 cross-continental CH<sub>4</sub> emissions from dry inland waters were converted into CO<sub>2</sub>-eq  
297 emissions by using the 100-year time horizon GWP factor of 34 (Myhre et al., 2013).

298

### 299       **3. Results and Discussion**

#### 300       ***3.1 Contrasting CH<sub>4</sub> fluxes from dry inland waters and surrounding terrestrial areas***

301       CH<sub>4</sub> fluxes from dry sediments of inland waters and adjacent uphill (terrestrial)  
302 soils ranged from -8 to 352 mg CH<sub>4</sub> m<sup>-2</sup> d<sup>-1</sup>, with a median of 0.08 mg CH<sub>4</sub> m<sup>-2</sup> d<sup>-1</sup> and  
303 an interquartile range (IQR) of 4.1 mg CH<sub>4</sub> m<sup>-2</sup> d<sup>-1</sup> (mean ± standard deviation (SD): 20  
304 ± 60 mg CH<sub>4</sub> m<sup>-2</sup> d<sup>-1</sup>) (Figure 2). CH<sub>4</sub> uptake was found in 51 uphill soil regions (57%)  
305 and 21 dry inland water regions (23%) (Figure 2D – see Figure 2E and F for system

306 type and climate zones). Variability of CH<sub>4</sub> fluxes was larger among dry inland water  
307 sediments than among uphill soils (Figure 2A). Uphill sites tend to be drained/dry and  
308 oxic, which represents unfavorable conditions for CH<sub>4</sub> production but favorable  
309 conditions for CH<sub>4</sub> consumption (von Fischer and Hedin, 2007). On the other hand,  
310 exposed inland-water sediments may sometimes be fully desiccated, showing little or no  
311 CH<sub>4</sub> production, or waterlogged with potential anoxia supporting CH<sub>4</sub> production and  
312 emission (Koschorreck, 2000). While CO<sub>2</sub> emissions from dry inland waters tend to be  
313 lower than those from uphill soils (Almeida et al., 2019; Catalán et al., 2014; Jin et al.,  
314 2016; Keller et al., 2020; von Schiller et al., 2014), the pattern we observed for CH<sub>4</sub> was  
315 opposite. Average CH<sub>4</sub> emissions from dry inland waters were significantly higher than  
316 those from adjacent uphill soils (Figure 2A; Table 1) (mean ± SD and median – IQR,  
317 respectively; dry inland water: 40 ± 80 mg CH<sub>4</sub> m<sup>-2</sup> d<sup>-1</sup>, and 1 – 28.4 mg CH<sub>4</sub> m<sup>-2</sup> d<sup>-1</sup>;  
318 uphill soil: 1 ± 4 mg CH<sub>4</sub> m<sup>-2</sup> d<sup>-1</sup>, and -0.07 – 1.1 mg CH<sub>4</sub> m<sup>-2</sup> d<sup>-1</sup>; GLMM:  $t = -9.61$ ,  $p <$   
319 0.001). The difference in CH<sub>4</sub> emissions from the two different regions may be  
320 attributed to differences in moisture content as well as quality and quantity of organic  
321 matter (Dalal et al., 2008; Serça et al., 2016; Serrano-Silva et al., 2014). When air-  
322 exposed sediments are still wet, anoxia generally prevails below the upper few  
323 millimeters of the sediment (Koschorreck and Darwich, 2003), thereby sustaining CH<sub>4</sub>  
324 production. When sediments start to dry out, CH<sub>4</sub> production through organic matter  
325 decomposition can still take place in anoxic microhabitats (Dalal et al., 2008;  
326 Koschorreck, 2000; Serrano-Silva et al., 2014). As exposed sediments of inland waters  
327 dry out further, newly formed fractures ease the contact of deeper sediment layers with  
328 atmospheric oxygen (Fromin et al., 2010; Kosten et al., 2018; Paranaíba et al., 2020).  
329 The expansion of the oxic layer in the sediment provokes changes in microbial  
330 communities and their activity (Borken and Matzner, 2009; Jin et al., 2016; Rodrigo et

331 al., 1997), favoring aerobic metabolisms (e.g., CH<sub>4</sub> oxidation; Jäckel et al., 2001;  
332 Koschorreck, 2000), and eventually leading to a reduction in CH<sub>4</sub> emissions (Kosten et  
333 al., 2018; Paranaíba et al., 2020). Furthermore, the microbial community in water-  
334 stressed sediments is expected to desiccate (Borken and Matzner, 2009; Jin et al., 2016;  
335 Rodrigo et al., 1997), which can be expected to diminish the potential of CH<sub>4</sub>  
336 production likely contributing to the wide range in CH<sub>4</sub> fluxes from dry inland-water  
337 sediments. The importance of moisture content in regulating CH<sub>4</sub> emission is further  
338 exemplified by the mean moisture content being consistently higher in dry inland-water  
339 sediments than in uphill soils across all systems globally (mean ± SD; dry inland water:  
340 33.1 ± 21.4%, uphill soil: 17 ± 9.4%; GLMM:  $t = -7.03$ ,  $p < 0.001$ ), corresponding with  
341 the generally higher CH<sub>4</sub> emissions from the dry inland-water sediments. Mean organic  
342 matter content, however, was similar for the two regions (mean ± SD; dry inland water:  
343 7.9 ± 7%, uphill soil: 8.2 ± 7.5%; GLMM:  $t = 0.19$ ,  $p = 0.84$ ).

344

### 345 ***3.2 Dry inland waters CH<sub>4</sub> flux variability across aquatic systems and climate zones***

346 No statistical differences in CH<sub>4</sub> fluxes were found between the different types  
347 of dry inland water systems (GLMM,  $F = 0.63$ ,  $p = 0.59$  – see Table S1 for pairwise  
348 comparisons), due to the relatively high variability among sites within each type (Figure  
349 2B; Table 1). Dry inland water sediments were a source of CH<sub>4</sub> in almost all cases,  
350 while adjacent uphill soils could be either a source or a sink of CH<sub>4</sub>, depending on the  
351 site (Figure 2E). Dry inland water CH<sub>4</sub> fluxes were, on average (± SD), 48 ± 91 mg CH<sub>4</sub>  
352 m<sup>-2</sup> d<sup>-1</sup> ( $n = 45$ ; median – IQR: 2.3 – 48.2 mg CH<sub>4</sub> m<sup>-2</sup> d<sup>-1</sup>) in lakes, 38 ± 63 mg CH<sub>4</sub> m<sup>-2</sup>  
353 d<sup>-1</sup> ( $n = 16$ ; median – IQR: 0.7 – 84 mg CH<sub>4</sub> m<sup>-2</sup> d<sup>-1</sup>) in ponds, 36 ± 78 mg CH<sub>4</sub> m<sup>-2</sup> d<sup>-1</sup>  
354 ( $n = 19$ ; median – IQR: 0.08 – 13.9 mg CH<sub>4</sub> m<sup>-2</sup> d<sup>-1</sup>) in reservoirs, and 7 ± 17 mg CH<sub>4</sub>  
355 m<sup>-2</sup> d<sup>-1</sup> ( $n = 9$ ; median – IQR: 0.1 – 3.5 mg CH<sub>4</sub> m<sup>-2</sup> d<sup>-1</sup>) in streams (Figure 2B; Table 1).

356 The lower CH<sub>4</sub> flux rate from dry streams corresponded with their significantly lower  
357 mean ( $\pm$  SD) moisture and organic matter content when compared to lakes, ponds and  
358 reservoirs (moisture content: streams:  $20 \pm 27\%$ , lakes:  $31 \pm 20\%$ , ponds:  $52 \pm 21\%$ ,  
359 reservoirs:  $27 \pm 10\%$ ; GLMM,  $F = 6.25$ ,  $p = 0.0006$  – see Table S2 for pairwise  
360 comparisons; organic matter content: streams:  $1 \pm 1\%$ , lakes:  $9 \pm 8\%$ , ponds:  $8 \pm 4\%$ ,  
361 reservoirs:  $9 \pm 6\%$ ; GLMM,  $F = 3.48$ ,  $p = 0.01$  – see Table S3 for pairwise  
362 comparisons). In fact, dry sediments of rivers and streams tend to have less organic  
363 matter content than dry sediments of lentic water bodies (Gómez-gener et al., 2015).  
364 Rivers and streams are more sensitive to variations in hydrological cycles (i.e., are  
365 subject to high and recurrent water stress). In addition, water flow erodes fine-grained  
366 sediment, which hinders organic matter accumulation at the margins of these systems  
367 (Boix-Fayos et al., 2015; Gómez-Gener et al., 2016).

368 The CH<sub>4</sub> fluxes presented here were higher than values reported for individual  
369 dry inland water CH<sub>4</sub>-emission in earlier studies conducted in different aquatic systems  
370 (Table 1). We can only speculate about the underlying reason, which may be related to  
371 drier conditions or low (quality) organic matter content found in the systems from  
372 earlier studies. For instance, the mean  $\pm$  SD of organic matter content found in 16  
373 ephemeral streams by Gallo et al. (2014) was  $3 \pm 2.7\%$ , and mean  $\pm$  SD dry CH<sub>4</sub>  
374 emission was  $0.4 \pm 0.5$  mg CH<sub>4</sub> m<sup>-2</sup> d<sup>-1</sup>, which is both considerably lower than the  
375 values we found.

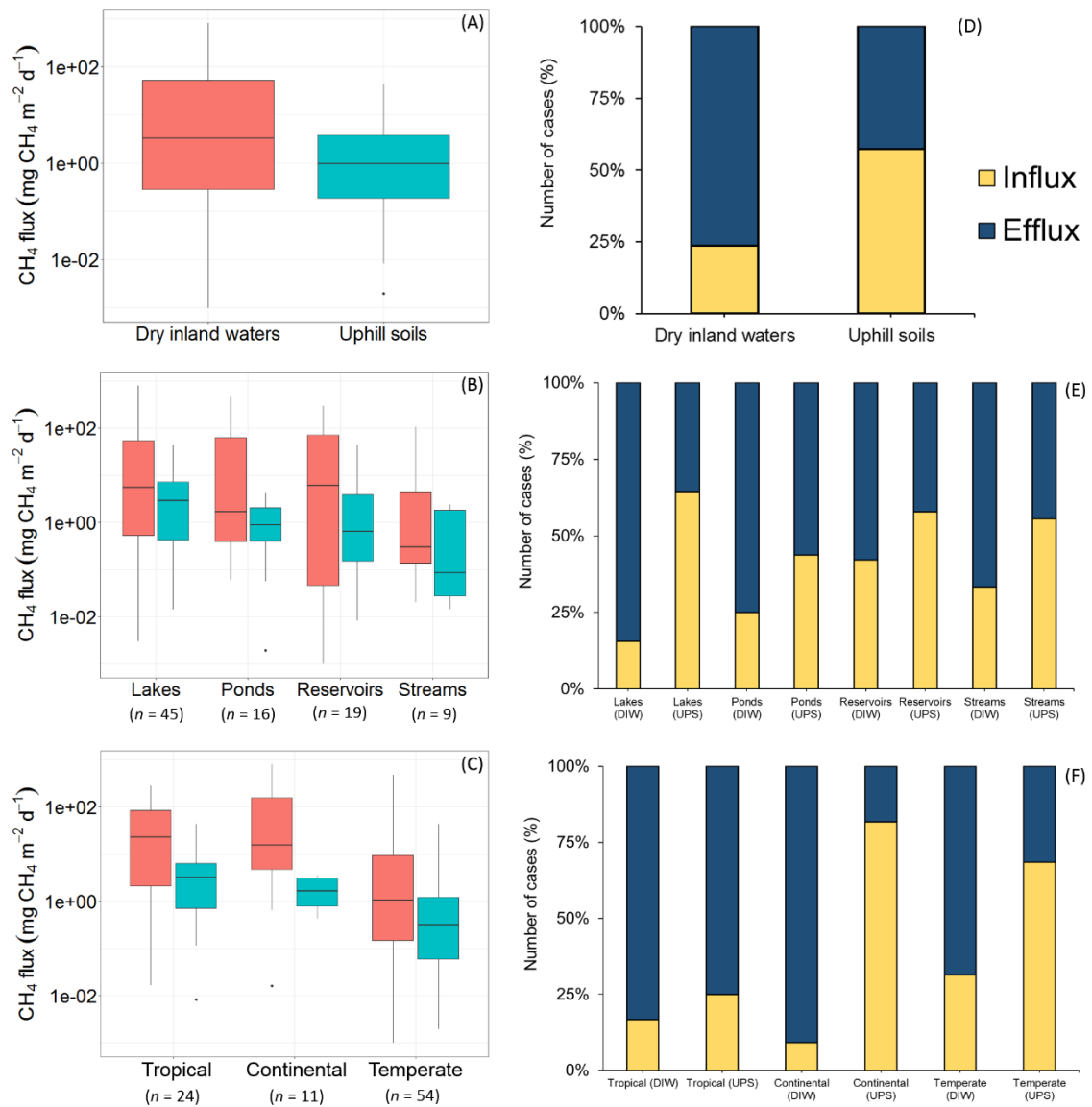
376 The CH<sub>4</sub> fluxes per square meter from dry inland waters were lower than those  
377 from surface waters reported in the literature (Table 1). This may be related to lower  
378 oxygen availability in submerged sediments possibly leading to higher CH<sub>4</sub> production  
379 and lower CH<sub>4</sub> consumption. In addition, the littoral regions of streams and reservoirs  
380 tend to be depleted in labile organic matter due to frequent water level changes, which

381 hampers the production of CH<sub>4</sub> in these regions (Dalal et al., 2008; Serrano-Silva et al.,  
382 2014).

383 No statistical differences in dry inland water CH<sub>4</sub> fluxes were found between  
384 climate zones (GLMM,  $F = 1.41$ ,  $p = 0.22$  – see Table S4 for pairwise comparisons),  
385 again likely due to the substantial variation in fluxes within climate zones. CH<sub>4</sub> efflux  
386 prevailed in dry inland-water sediments across climate zones, while CH<sub>4</sub> influx was  
387 more evident in adjacent uphill soils (except for soils from tropical zones) (Figure 2F).  
388 Mean ( $\pm$  SD) dry inland water CH<sub>4</sub> fluxes were  $96 \pm 128$  mg CH<sub>4</sub> m<sup>-2</sup> d<sup>-1</sup> ( $n = 11$ ;  
389 median – IQR:  $0.5 - 232.1$  mg CH<sub>4</sub> m<sup>-2</sup> d<sup>-1</sup>) in continental zones,  $54 \pm 77$  mg CH<sub>4</sub> m<sup>-2</sup> d<sup>-1</sup>,  
390 <sup>1</sup> ( $n = 24$ ; median – IQR:  $0.08 - 87.5$  mg CH<sub>4</sub> m<sup>-2</sup> d<sup>-1</sup>) in tropical zones, and  $22 \pm 58$  mg  
391 CH<sub>4</sub> m<sup>-2</sup> d<sup>-1</sup> ( $n = 54$ ; median – IQR:  $-0.03 - 3.7$  mg CH<sub>4</sub> m<sup>-2</sup> d<sup>-1</sup>) in temperate zones  
392 (Figure 2C). Interestingly, the highest emissions obtained in our study were observed at  
393 sampling sites located in the continental zone (mean  $\pm$  SD:  $352 \pm 150$  mg CH<sub>4</sub> m<sup>-2</sup> d<sup>-1</sup>;  
394  $293 \pm 351$  mg CH<sub>4</sub> m<sup>-2</sup> d<sup>-1</sup>; and  $232 \pm 201$  mg CH<sub>4</sub> m<sup>-2</sup> d<sup>-1</sup>), which ended up determining  
395 the higher mean CH<sub>4</sub> emission attributed to continental zones. In addition, local  
396 characteristics not captured in our sampling design (e.g., surrounding land use, trophic  
397 state, microbial community structure, timing of atmospheric exposure) rather than  
398 regional characteristics (e.g., mean annual temperature) may be responsible for both the  
399 high CH<sub>4</sub> emission rates and the high variability observed in our measurements. Mean  
400 sediment moisture content was similar among climate zones (GLMM,  $F = 2.50$ ,  $p =$   
401  $0.09$ ; see Table S5 for pairwise comparisons). The mean moisture content ( $\pm$  SD) in dry  
402 sediments was  $37 \pm 22\%$  in temperate zones,  $32 \pm 27\%$  in continental zones, and  $25 \pm$   
403  $14\%$  in tropical zones. The highest mean ( $\pm$  SD) organic matter content was observed in  
404 dry sediments of tropical zones ( $11 \pm 9\%$ ), followed by those in temperate ( $7 \pm 5\%$ ) and

405 continental zones ( $4 \pm 5\%$ ) (GLMM,  $F = 5.37$ ,  $p = 0.006$  – see Table S6 for pairwise  
 406 comparisons).

407



408

409 **Figure 2** | Boxplot of  $\text{CH}_4$  fluxes ( $\text{mg CH}_4 \text{ m}^{-2} \text{ d}^{-1}$ ) from dry inland waters (red boxes)  
 410 and adjacent uphill soils (cyan boxes) (A); in different types of aquatic systems (B); and  
 411 different climate zones (C). Number of cases of  $\text{CH}_4$  influx (yellow bars) and efflux  
 412 (blue bars) from dry inland waters (DIW) and adjacent uphill soils (UPS) (D); in  
 413 different types of aquatic systems (E); and different climate zones (F). In A, B and C,

414 the y-axes are presented as logarithmic scale ( $\log_{10}$ ), the lines within the boxes indicate  
 415 the median, the boxes delimit the 25<sup>th</sup> and 75<sup>th</sup> percentiles, and the whiskers delimit the  
 416 5<sup>th</sup> and 95<sup>th</sup> percentiles.

417 **Table 1 | Upper part:** Mean  $\pm$  standard deviation of CH<sub>4</sub> fluxes (mg CH<sub>4</sub> m<sup>-2</sup> d<sup>-1</sup>) from  
 418 dry inland waters (dry sediments) and adjacent uphill soils among lakes, ponds,  
 419 reservoirs, and streams. **Middle part:** Mean  $\pm$  standard deviation of CH<sub>4</sub> fluxes (mg  
 420 CH<sub>4</sub> m<sup>-2</sup> d<sup>-1</sup>) from other dry inland waters (documented in the literature). **Bottom part:**  
 421 Global mean  $\pm$  standard deviation of CH<sub>4</sub> fluxes (mg CH<sub>4</sub> m<sup>-2</sup> d<sup>-1</sup>) from surface waters  
 422 of lakes, ponds, reservoirs, and streams (documented in the literature).

System type	CH <sub>4</sub> flux (mg CH <sub>4</sub> m <sup>-2</sup> d <sup>-1</sup> )	Reference
<b>Lakes (n = 45)</b>		
Dry sediment	48 $\pm$ 91	
Uphill soil	1 $\pm$ 5	
<b>Ponds (n = 16)</b>		
Dry sediment	38 $\pm$ 63	
Uphill soil	0.3 $\pm$ 1	
<b>Reservoirs (n = 19)</b>		
Dry sediment	36 $\pm$ 78	This study
Uphill soil	2 $\pm$ 4	
<b>Streams (n = 9)</b>		
Dry sediment	7 $\pm$ 17	
Uphill soil	0.2 $\pm$ 0.7	
<b>All systems (n = 89)</b>		
Dry sediment	40 $\pm$ 80	
Uphill soil	1 $\pm$ 4	
<b>Lake (Brazil)</b>	1.4 $\pm$ 0.15 (Amazonian floodplain)	Koschorreck, 2000
<b>Ponds (Spain)</b>	4.8 $\pm$ 3.8 (Dry bed)	Obrador et al. 2018
<b>Reservoir (Brazil)</b>	0.9 $\pm$ 6.9 (Drawdown)	Amorim et al. 2019
<b>Reservoir (China)</b>	7 $\pm$ 8.9 (Drawdown)	Chen et al. 2011
<b>Reservoir (China)</b>	4 $\pm$ 1.5 (Drawdown)	Yang et al. 2012
<b>Reservoir (China)</b>	7.7 $\pm$ 5 (Drawdown)	Hao et al. 2019
<b>Reservoir (Laos)</b>	27 $\pm$ 36 (Drawdown)	Serça et al. 2016
<b>Reservoir (Germany)</b>	4.1 <sup>a</sup> (Drawdown)	Marcé et al. 2019
<b>Reservoir (Germany)</b>	7.2 <sup>a</sup> (Drawdown)	Marcé et al. 2019
<b>Reservoir (Spain)</b>	0 (Drawdown)	Marcé et al. 2019
<b>Reservoir (Spain)</b>	4.1 <sup>a</sup> (Drawdown)	Marcé et al. 2019
<b>Reservoir (Spain)</b>	0.3 <sup>a</sup> (Drawdown)	Marcé et al. 2019
<b>Streams (United States)</b>	0.4 $\pm$ 0.5 (Dry river bed)	Gallo et al. 2014
<b>Streams (Spain)</b>	3.2 $\pm$ 0.9 (Dry river and impoundment beds)	Gómez-Gener et al. 2015
<b>Global CH<sub>4</sub> flux rates from surface waters (mg CH<sub>4</sub> m<sup>-2</sup> d<sup>-1</sup>)</b>		

<b>Lakes</b>	153 ± 293	Rosentreter et al. 2021
<b>Ponds</b>	12 ± 30	Holgerson and Raymond 2016
<b>Reservoirs</b>	165 ± 369	Rosentreter et al. 2021
<b>Streams</b>	112 ± 425	Rosentreter et al. 2021

<sup>a</sup> Mean values

### 423 3.3 Drivers of CH<sub>4</sub> fluxes

424 The fixed effects resulting from the GLMM modeling on dry inland water CH<sub>4</sub>  
425 fluxes explained 23% of the total variance (marginal R squared, R<sup>2</sup>m), and fixed and  
426 random effects together explained 57% of the total variance (conditional R squared,  
427 R<sup>2</sup>c) (Table 2). Organic matter content and the interaction between organic matter  
428 content and sediment temperature were the strongest predictors of CH<sub>4</sub> fluxes from dry  
429 inland waters ( $p < 0.001$ ; Figure S1; Table 2), followed by moisture, conductivity ( $p <$   
430  $0.01$ ; Figure S1; Table 2), elevation and the interaction between moisture and organic  
431 matter content ( $p < 0.05$ ; Figure S1; Table 2). This suggests that local sediment  
432 characteristics rather than regional characteristics such as annual mean temperature  
433 drive CH<sub>4</sub> emissions, which agrees with findings for dry inland-water CO<sub>2</sub> emissions  
434 (Keller et al., 2020) (Figure S1; Table 2). However, the particular drivers of CO<sub>2</sub> and  
435 CH<sub>4</sub> emissions differed. Most pronounced was the positive relationship between organic  
436 matter content and CO<sub>2</sub> emission (Keller et al., 2020) and the negative relationship  
437 between CH<sub>4</sub> and organic matter content reported here. The relationship between  
438 organic matter content and CH<sub>4</sub> emission was more complex than the negative GLMM  
439 coefficient may suggest, given that high CH<sub>4</sub> emissions were measured along the entire  
440 organic matter gradient, particularly at intermediate moisture contents (Figure 3).  
441 Although not investigated here, the quality of available organic matter may likely be the  
442 controlling factor of CH<sub>4</sub> production in our dry inland water sediments (Dalal et al.,  
443 2008; Serça et al., 2016; Serrano-Silva et al., 2014; Strom et al., 2003). The quality of  
444 organic matter depends on its origin and may be of particular importance in the context

445 of this study regarding the frequency of sediment exposure to the atmosphere. The more  
446 frequently a sediment is exposed to the atmosphere, the less labile its organic matter  
447 tends to be (Dalal et al., 2008; Serrano-Silva et al., 2014). This might suggest that lower  
448 CH<sub>4</sub> production rates can be expected from exposed sediments in aquatic systems that  
449 experience frequent water level fluctuations than from those with a generally more  
450 constant water level (e.g., reservoirs and lakes, respectively; Table 1). The transition  
451 from wet to drying stage triggers microbial processes responsible for organic matter  
452 breakdown (Fromin et al., 2010; Jin et al., 2016) that in turn boost CH<sub>4</sub> emissions,  
453 mainly in the first hours and/or days after the transition (Jin et al., 2016; Koschorreck,  
454 2000; Kosten et al., 2018; Paranaíba et al., 2020). The drying-rewetting history of the  
455 sediments in our study may therefore have influenced the observed relationships  
456 between bulk organic matter content and CH<sub>4</sub> fluxes.

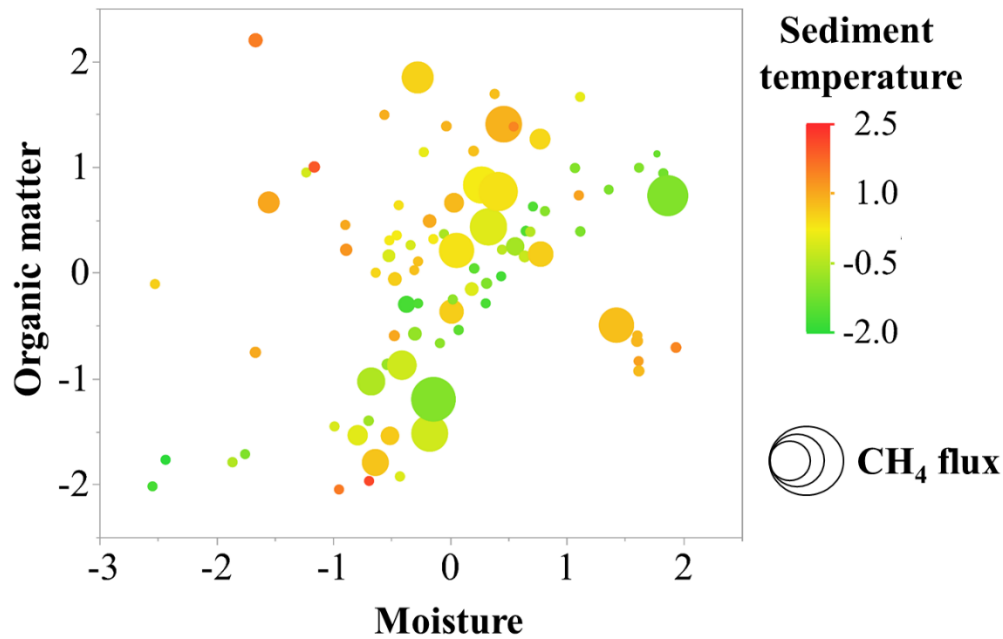
457         We found a positive effect of moisture on dry inland water CH<sub>4</sub> fluxes (Figure  
458 S1; Table 2), which may be related to the fact that the moisture content regulates  
459 microbial activity in these water-stressed marginal regions (Baldwin and Mitchell,  
460 2000; Manzoni et al., 2012; Sponseller, 2007). CH<sub>4</sub>-producing microorganisms thrive in  
461 anoxic conditions. Moisture permits anoxic microhabitats and reduces the depth to  
462 which oxygen penetrates the sediments. Increased sediment moisture content therefore  
463 favors the presence and maintenance of methanogenic (i.e., CH<sub>4</sub>-producing) microbial  
464 communities and likely reduces CH<sub>4</sub> oxidation, which may help to explain our finding  
465 that moisture content and CH<sub>4</sub> emissions were positively correlated (Dalal et al., 2008;  
466 Koschorreck, 2000; Serrano-Silva et al., 2014). Ultimately, the positive effect of  
467 sediment conductivity and land elevation on dry inland water CH<sub>4</sub> fluxes may be  
468 associated with the influence of regional-to-local underlying characteristics that are not  
469 explicitly included in our analysis. For example, a water body's trophic status, type of

470 surrounding land cover (e.g., natural vegetation, crops, urbanization), and a sediment's  
 471 organic matter quality, microbial community structure and timing and history of its  
 472 exposure to the atmosphere may affect CH<sub>4</sub> dynamics (Atekwana et al., 2004; Dalal et  
 473 al., 2008; Datry et al., 2018; Lischeid and Kalettka, 2012; Onandia et al., 2021; Serrano-  
 474 Silva et al., 2014).

475 **Table 2** | Results from the GLMM describing CH<sub>4</sub> flux from dry inland waters.  
 476 Standardized coefficients ( $\beta$ ), standard error (SE), *t*-values, 95% confidence intervals  
 477 (CI), marginal R squared (R<sup>2</sup><sub>m</sub>), and conditional R squared (R<sup>2</sup><sub>c</sub>) are reported. Moisture  
 478 and elevation data were transformed by cubic root, organic matter content and  
 479 conductivity were log<sub>10</sub>-transformed, and all predictor variables were z-transformed  
 480 before analysis. The colon indicates interaction between the respective variables.

Input variable	CH <sub>4</sub> flux			
	$\beta$	SE	<i>t</i> -value	CI
(Intercept)	3.53	0.30	11.64	2.93 – 4.12
<b>Interaction</b> (Organic matter:Sediment temperature)	0.39	0.10	3.69	0.18 – 0.59
<b>Organic matter</b>	-0.54	0.15	-3.55	-0.85 – -0.24
<b>Moisture</b>	0.49	0.15	3.20	0.19 – 0.79
<b>Conductivity</b>	0.37	0.12	3.01	0.12 – 0.61
<b>Elevation</b>	0.35	0.17	1.98	0.004 – 0.7
<b>Interaction</b> (Moisture:Organic matter)	-0.20	0.10	-2.01	-0.41 – -0.006
<b>R<sup>2</sup><sub>m</sub></b>	0.23			
<b>R<sup>2</sup><sub>c</sub></b>	0.57			

481



482

483 **Figure 3** | Response of dry inland water CH<sub>4</sub> fluxes (mg CH<sub>4</sub> m<sup>-2</sup> d<sup>-1</sup>) to the interaction  
 484 between organic matter (%), moisture (%) and sediment temperature (°C) (all z-  
 485 transformed) arising from the GLMM. Larger circles represent higher CH<sub>4</sub> flux values.

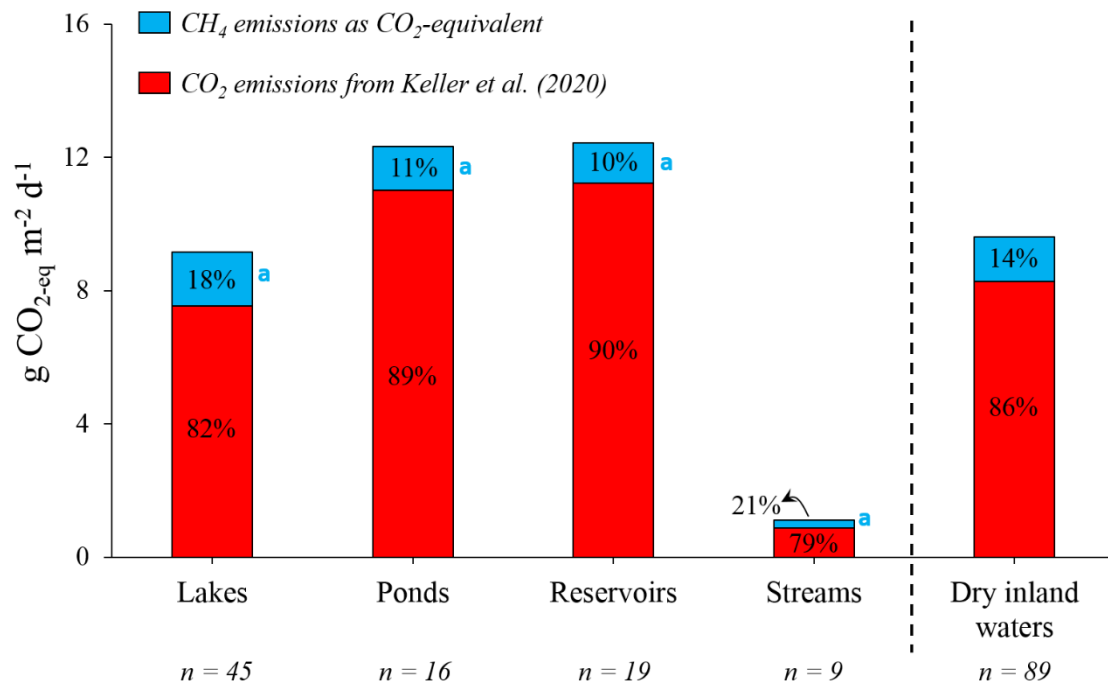
486

### 487 **3.4 Contribution of CH<sub>4</sub> to the CO<sub>2</sub>-equivalent cross-continental inland water fluxes**

488 Summing dry inland water CO<sub>2</sub> fluxes (Keller et al., 2020) with the CH<sub>4</sub> fluxes  
 489 presented here (as CO<sub>2</sub>-eq; assuming a GWP of 34 for CH<sub>4</sub> compared to CO<sub>2</sub>; Myhre et  
 490 al., 2013) resulted in a cross-continental mean (± SD) emission rate of 9.6 ± 17.4 g CO<sub>2</sub>-  
 491 eq m<sup>-2</sup> d<sup>-1</sup> (Figure 4), of which ~14% are attributed to CH<sub>4</sub>. This estimate represents  
 492 about 2.6 ± 4.7 (± SD) g C m<sup>-2</sup> d<sup>-1</sup>, which is about one order of magnitude higher than  
 493 the global organic C burial rate related to lakes, ponds, and reservoirs (~0.1 g C m<sup>-2</sup> d<sup>-1</sup>;  
 494 Mendonça et al., 2017). We found no statistical differences in CH<sub>4</sub> contribution to the  
 495 total CO<sub>2</sub>-eq emission between types of aquatic systems (mean ± SD; lakes = 9.2 ± 13 g  
 496 CO<sub>2</sub>-eq m<sup>-2</sup> d<sup>-1</sup>; ponds = 12.3 ± 11 g CO<sub>2</sub>-eq m<sup>-2</sup> d<sup>-1</sup>; reservoirs = 12.4 ± 29 g CO<sub>2</sub>-eq m<sup>-2</sup>  
 497 d<sup>-1</sup>; and streams = 1.1 ± 0.8 g CO<sub>2</sub>-eq m<sup>-2</sup> d<sup>-1</sup>; GLMM,  $F = 1.01$ ,  $p = 0.39$  – see Table

498 S7 for pairwise comparisons) (Figure 4). This can likely be explained by the large  
499 variability in climate conditions, trophic state, sediment type and water level  
500 fluctuations, within and between the different types of systems. Therefore, other factors  
501 likely outplay differences arising from the type of aquatic system. As a consequence,  
502 the contribution of CH<sub>4</sub> to the total GHG emission estimate did not significantly vary  
503 among systems either; it ranged from 10% to 21% contribution to the total CO<sub>2</sub>-eq  
504 emission from dry inland waters (Figure 4).

505         Upscaling the mean dry inland water CH<sub>4</sub> flux rates from lakes, reservoirs,  
506 ponds and streams according to their respective global surface areas revealed that  $3.6 \pm$   
507  $0.4$  ( $\pm$  standard error of the mean; SEM) Tg CH<sub>4</sub> evade from the dry sediments of inland  
508 waters to the atmosphere annually (Table 3). This represents approximately 2.4% ( $\pm$   
509 0.2%; SEM) of the global CH<sub>4</sub> emission estimate attributed to water surfaces of lentic  
510 and lotic inland water ecosystems ( $0.15 \text{ Pg CH}_4 \text{ y}^{-1}$ ; Rosentreter et al., 2021).  
511 Converting our cross-continental CH<sub>4</sub> emission from dry inland waters to C emission  
512 indicates that CH<sub>4</sub> adds  $\sim 2.7$  ( $\pm 0.3$ ; SEM) Tg C  $\text{y}^{-1}$  (or 0.07%) to the current global C  
513 emission estimate from inland waters ( $3.9 \text{ Pg C y}^{-1}$ ; Drake et al., 2018) (Table 3).



514

515 **Figure 4** | Cross-continental mean CO<sub>2</sub>-equivalent emission rates (CH<sub>4</sub> – blue; CO<sub>2</sub> –  
516 red; g CO<sub>2</sub>-eq m<sup>-2</sup> d<sup>-1</sup>) from dry inland waters (far-right bar) divided by the different  
517 types of aquatic systems (lakes, ponds, reservoirs, and streams). CO<sub>2</sub> flux measurements  
518 were obtained from Keller et al. (2020) and were associated with the CH<sub>4</sub> flux  
519 measurements collected at the same sampling sites. CH<sub>4</sub> fluxes were converted into  
520 CO<sub>2</sub>-equivalents by multiplying the mass-based CH<sub>4</sub> flux by 34, according to the 100-  
521 year GWP (Myhre et al., 2013). Percentage values represent the contribution of each gas  
522 to the cross-continental average emission rate in each type of aquatic system. Letter “a”  
523 indicates no statistical difference in CH<sub>4</sub> contribution between the types of aquatic  
524 systems.

525 **Table 3** | Cross-continental mean fluxes ( $\pm$  standard error of the mean;  $\text{mg CH}_4 \text{ m}^{-2} \text{ d}^{-1}$ ) and cross-continental estimates of dry inland water  $\text{CH}_4$   
 526 emissions ( $\text{Tg CH}_4 \text{ y}^{-1}$ ,  $\text{Pg CO}_2\text{-eq y}^{-1}$ , and  $\text{Tg C y}^{-1}$ ) by different types of aquatic systems.

<b>System type</b>	<b>Area of exposed aquatic sediments during one year <sup>a</sup></b>	<b>CH<sub>4</sub> emission rate</b>	<b>Cross-continental CH<sub>4</sub> emission</b>	<b>Cross-continental CH<sub>4</sub> emission in CO<sub>2</sub> equivalents</b>	<b>Cross-continental CH<sub>4</sub> emission as C emission</b>
	<b>(km<sup>2</sup>)</b>	<b>(mg CH<sub>4</sub> m<sup>-2</sup> d<sup>-1</sup>)</b>	<b>(Tg CH<sub>4</sub> y<sup>-1</sup>)</b>	<b>(Pg CO<sub>2</sub>-eq y<sup>-1</sup>)</b>	<b>(Tg C y<sup>-1</sup>)</b>
<b>Lakes and reservoirs</b>	187,542 (Marcé et al., 2019)	44 ± 10.9	3.1 ± 0.7	0.1 ± 0.02	2.3 ± 0.5
<b>Ponds</b>	18,390 (Marcé et al., 2019)	38 ± 15.7	0.26 ± 0.1	0.009 ± 0.003	0.2 ± 0.08
<b>Streams and rivers</b>	84,461 (Raymond et al., 2013)	7 ± 5.6	0.21 ± 0.1	0.007 ± 0.006	0.16 ± 0.13
<b>Total</b>	290,393		3.6 ± 0.4	0.11 ± 0.01	2.7 ± 0.3

527 <sup>a</sup> *Seasonal and permanent exposure*

#### 528 4. Conclusions, implications and future perspectives

529 This study provides the first cross-continental assessment of CH<sub>4</sub> fluxes from  
530 dry inland waters based on *in situ* measurements. We found that 14% of the cross-  
531 continental CO<sub>2</sub>-eq emissions from dry inland waters can be attributed to CH<sub>4</sub>. Our  
532 estimate comes with uncertainties as the number of aquatic systems and climate zones  
533 included in this study were non-uniformly represented (i.e., arid and polar regions were  
534 not represented at all, and temperate zones were overrepresented), and given the large  
535 variation in dry inland water CH<sub>4</sub> fluxes observed within the different types of aquatic  
536 systems and climate zones studied here. Moreover, our estimates are solely related to  
537 gaseous C species (CH<sub>4</sub> and CO<sub>2</sub>) emissions and do not account for nitrous oxide (N<sub>2</sub>O)  
538 emissions which is an important GHG in these systems as well (Arce et al., 2018). In  
539 addition, our global estimate of CH<sub>4</sub> emissions from dry inland waters may be an  
540 underestimation because we likely underestimated the global surface area of dry inland  
541 waters. While we used a surface area of 290,393 km<sup>2</sup> for our upscaling exercise, another  
542 study that does not differentiate between types of aquatic systems and included  
543 wetlands concluded that this area is considerably higher (806,321 km<sup>2</sup> – Pekel et al.  
544 (2016)). Also, during our sampling, we likely generally missed emission peaks (i.e., hot  
545 moments of emission) that can occur at the onset of drying (Jin et al., 2016;  
546 Koschorreck, 2000; Kosten et al., 2018; Paranaíba et al., 2020). Ultimately, while our  
547 estimates account for a good portion of the variability related to weather conditions  
548 (since we sampled CH<sub>4</sub> fluxes and environmental parameters across a wide range of  
549 locations and climate zones), our estimates do not consider CH<sub>4</sub> fluxes occurring under  
550 extreme weather events (e.g., rainy days, snowy days), which therefore represents a  
551 knowledge gap in this area of research and certainly deserves further research.

552 While the global CH<sub>4</sub> emission from dry inland waters may be small compared  
553 to total aquatic (wet and dry, CO<sub>2</sub> and CH<sub>4</sub>) emissions, for individual systems, CH<sub>4</sub>  
554 emission from dry sediments can be important (Jin et al., 2016). Dry inland-water  
555 sediments occupy a temporally varying fraction of aquatic systems due to cycles of  
556 rising and falling water levels. Hence, the contribution of dry-sediment CH<sub>4</sub>, CO<sub>2</sub> and  
557 N<sub>2</sub>O emissions to the total emission also varies through time (Almeida et al., 2019; Arce  
558 et al., 2018; Keller et al., 2021; Kosten et al., 2018; Paranaíba et al., 2020). The time-  
559 integrated contribution of dry sediment to total inland water emissions is likely to  
560 increase in the future as drought events are becoming more frequent and more intense.  
561 As a result of this and ongoing widespread direct consumptive water uses, large areas of  
562 marginal sediments from aquatic systems worldwide will be exposed to the atmosphere  
563 (Pekel et al., 2016; Steward et al., 2012; Wurtsbaugh et al., 2017). We argue that future  
564 work on aquatic GHG emissions needs to take CH<sub>4</sub>, CO<sub>2</sub> and N<sub>2</sub>O emissions from these  
565 dynamic wet-dry regions into account in order to further improve our estimates of the  
566 global GHG budget of inland waters. Such gained insights into the environmental  
567 processes that produce and consume GHGs will enable improved predictions of changes  
568 in atmospheric GHG concentrations under varying climate change scenarios.

569

## 570 **5. Acknowledgments**

571 This study was made possible thanks to an extensive collective effort of a global  
572 research network called dryflux ([www.ufz.de/dryflux](http://www.ufz.de/dryflux)). Many thanks to all those who  
573 provided assistance in the field. *In memory of Julia Howitt, who will be missed and*  
574 *always remembered by her colleagues, friends, and family.*

575

576 **6. Funding**

577 JRP and GQ were supported by the Coordenação de Aperfeiçoamento de Pessoal de  
578 Nível Superior (CAPES, Finance Code 001). ALi and SS were supported by the  
579 European Research Council under the European Union's Seventh Framework  
580 Programme (FP7/2007-2013)/ERC grant agreement n° 336642. MK and PK were  
581 supported by the German Research Foundation (DFG, KO1911/6-1) and the Federal  
582 Ministry for Education and Research of Germany within the project SevaMod  
583 (01DK17022). AMA and FR gratefully acknowledge continuous funding through the  
584 Research Productivity Grant provided by the Conselho Nacional de Desenvolvimento  
585 Científico e Tecnológico – CNPq (process n° 312772/2020-3 and 310033/2017-9). ALa  
586 was supported by the Estonian Research Council grant PSG32. EIR was supported by  
587 Estonian Research Council grant PUT1598 and IUT 21-02. DvS was supported by the  
588 project PURIFY (ACRP10-PURIFY-KR17AC0K13643) funded by the Austrian  
589 Government and the project Alter-C (PID2020-114024GB-C31) funded by MCIN/AEI  
590 /10.13039/501100011033. NC was supported by the European Union's Horizon 2020  
591 research and innovation programme under the Marie Skłodowska-Curie grant  
592 agreement n° 839709. GO was supported by the German Federal Ministry of Education  
593 and Research BMBF within the Collaborative Project “Bridging in Biodiversity Science  
594 – BIBS” n° 01LC1501A-H. RM participated through the project Alter-C (Spanish AEI  
595 ref. PID2020-114024GB-C32).

596

597 **The authors declare no competing interests.**

598

599       **7. References**

- 600    Aben, R.C.H., Barros, N., Van Donk, E., Frenken, T., Hilt, S., Kazanjian, G., Lamers,  
601       L.P.M., Peeters, E.T.H.M., Roelofs, J.G.M., De Senerpont Domis, L.N., Stephan,  
602       S., Velthuis, M., Van De Waal, D.B., Wik, M., Thornton, B.F., Wilkinson, J.,  
603       Delsontro, T., Kosten, S., 2017. Cross continental increase in methane ebullition  
604       under climate change. *Nat. Commun.* 8, 1–8. [https://doi.org/10.1038/s41467-017-](https://doi.org/10.1038/s41467-017-01535-y)  
605       01535-y
- 606    Abril, G., Guérin, F., Richard, S., Delmas, R., Galy-Lacaux, C., Gosse, P., Tremblay,  
607       A., Varfalvy, L., Dos Santos, M.A., Matvienko, B., 2005. Carbon dioxide and  
608       methane emissions and the carbon budget of a 10-year old tropical reservoir (Petit  
609       Saut, French Guiana). *Global Biogeochem. Cycles* 19, 1–16.  
610       <https://doi.org/10.1029/2005GB002457>
- 611    Akinwande, M.O., Dikko, H.G., Samson, A., 2015. Variance Inflation Factor: As a  
612       Condition for the Inclusion of Suppressor Variable(s) in Regression Analysis.  
613       *Open J. Stat.* 05, 754–767. <https://doi.org/10.4236/ojs.2015.57075>
- 614    Almeida, R., Paranaíba, J., Barbosa, Í., Sobek, S., Kosten, S., Linkhorst, A., Mendonça,  
615       R., Quadra, G., Roland, F., Barros, N., 2019. Carbon dioxide emission from  
616       drawdown areas of a Brazilian reservoir is linked to surrounding land cover.  
617       *Aquat. Sci.* 81. <https://doi.org/10.1007/s00027-019-0665-9>
- 618    Anderson, N.J., Heathcote, A.J., Engstrom, D.R., Ryves, D.B., Mills, K., Prairie, Y.T.,  
619       del Giorgio, P.A., Bennion, H., Turner, S., Rose, N.L., Jones, V.J., Solovieva, N.,  
620       Cook Shinneman, A., Umbanhowar, C.E., Fritz, S.C., Verschuren, D., Saros, J.E.,  
621       Russell, J.M., Bindler, R., Valero-Garcés, B., Edlund, M.B., Dietz, R.D., Myrbo,  
622       A.E., 2020. Anthropogenic alteration of nutrient supply increases the global  
623       freshwater carbon sink. *Sci. Adv.* 6, 1–8. <https://doi.org/10.1126/sciadv.aaw2145>
- 624    Arce, M.I., Von Schiller, D., Bengtsson, M.M., Hinze, C., Jung, H., Alves, R.J.E.,

625 Urich, T., Singer, G., 2018. Drying and rainfall shape the structure and functioning  
626 of nitrifying microbial communities in riverbed sediments. *Front. Microbiol.* 9, 1–  
627 17. <https://doi.org/10.3389/fmicb.2018.02794>

628 Atekwana, Estella A, Atekwana, Eliot A, Werkema, D.D., Allen, J.P., Smart, L.A.,  
629 Duris, J.W., Cassidy, D.P., Sauck, W.A., Rossbach, S., 2004. Evidence for  
630 microbial enhanced electrical conductivity in hydrocarbon-contaminated  
631 sediments. *Geophys. Res. Lett.* 31, 1–4. <https://doi.org/10.1029/2004GL021359>

632 Attermeyer, K., Grossart, H.P., Flury, S., Premke, K., 2017. Bacterial processes and  
633 biogeochemical changes in the water body of kettle holes - mainly driven by  
634 autochthonous organic matter? *Aquat. Sci.* 79, 675–687.  
635 <https://doi.org/10.1007/s00027-017-0528-1>

636 Baldwin, D.S., Mitchell, A.M., 2000. The effects of drying and re-flooding on the  
637 sediment and soil nutrient dynamics of lowland river-floodplain systems: a  
638 synthesis. *Regul. Rivers Res. Manag.* 16, 457–467. [https://doi.org/10.1002/1099-  
639 1646\(200009/10\)16:5<457::aid-rrr597>3.3.co;2-2](https://doi.org/10.1002/1099-1646(200009/10)16:5<457::aid-rrr597>3.3.co;2-2)

640 Bastviken, D., Cole, J., Pace, M., Tranvik, L., 2004. Methane emissions from lakes:  
641 Dependence of lake characteristics, two regional assessments, and a global  
642 estimate. *Global Biogeochem. Cycles* 18, 1–12.  
643 <https://doi.org/10.1029/2004GB002238>

644 Bastviken, D., Tranvik, L.J., Downing, J.A., Crill, P.M., Enrich-Prast, A., 2011.  
645 Freshwater methane emissions offset the continental carbon sink. *Science* (80-. ).  
646 331, 1–2. <https://doi.org/10.1126/science.1196808>

647 Bates, D., Mächler, M., Bolker, B.M., Walker, S.C., 2015. Fitting linear mixed-effects  
648 models using lme4. *J. Stat. Softw.* 67, 1–48. <https://doi.org/10.18637/jss.v067.i01>

649 Beaulieu, J.J., Balz, D.A., Birchfield, M.K., Harrison, J.A., Nietch, C.T., Platz, M.C.,

650 Squier, W.C., Waldo, S., Walker, J.T., White, K.M., Young, J.L., 2018. Effects of  
651 an Experimental Water-level Drawdown on Methane Emissions from a Eutrophic  
652 Reservoir. *Ecosystems* 21, 657–674. <https://doi.org/10.1007/s10021-017-0176-2>

653 Boix-Fayos, C., Nadeu, E., Quiñonero, J.M., Martínez-Mena, M., Almagro, M., De  
654 Vente, J., 2015. Sediment flow paths and associated organic carbon dynamics  
655 across a Mediterranean catchment. *Hydrol. Earth Syst. Sci.* 19, 1209–1223.  
656 <https://doi.org/10.5194/hess-19-1209-2015>

657 Borken, W., Matzner, E., 2009. Reappraisal of drying and wetting effects on C and N  
658 mineralization and fluxes in soils. *Glob. Chang. Biol.* 15, 808–824.  
659 <https://doi.org/10.1111/j.1365-2486.2008.01681.x>

660 Catalán, N., Schiller, D. Von, Marcé, R., Koschorreck, M., Gomez-gener, L., Obrador,  
661 B., 2014. Carbon dioxide efflux during the flooding phase of temporary ponds.  
662 *Limnetica* 33, 349–360.

663 Clair, T.A., Ehrman, J.M., 1996. Variations in Discharge and Dissolved Organic Carbon  
664 and Nitrogen Export from Terrestrial Basins with Changes in Climate : A Neural  
665 Network Approach. *Limnol. Oceanogr.* 41, 921–927.

666 Cole, J.J., Caraco, N.F., 1998. Atmospheric exchange of carbon dioxide in a low-wind  
667 oligotrophic lake measured by the addition of SF<sub>6</sub>. *Limnol. Oceanogr.* 43, 647–  
668 656. <https://doi.org/10.4319/lo.1998.43.4.0647>

669 Cole, J.J., Prairie, Y.T., Caraco, N.F., McDowell, W.H., Tranvik, L.J., Striegl, R.G.,  
670 Duarte, C.M., Kortelainen, P., Downing, J.A., Middelburg, J.J., Melack, J., 2007.  
671 Plumbing the global carbon cycle: Integrating inland waters into the terrestrial  
672 carbon budget. *Ecosystems* 10, 171–184. <https://doi.org/10.1007/s10021-006->  
673 9013-8

674 Dalal, R.C., Allen, D.E., Livesley, S.J., 2008. Magnitude and biophysical regulators of

675 methane emission and consumption in the Australian agricultural , forest , and  
676 submerged landscapes : a review. *Plant Soil* 309, 43–76.  
677 <https://doi.org/10.1007/s11104-007-9446-7>

678 Datry, T., Foulquier, A., Corti, R., Tockner, K., Gessner, M.O., Stubbington, R., Allen,  
679 D.C., Altermatt, F., Arce, M.I., Arnon, S., Banas, D., Beller, E., Blanchette, M.L.,  
680 Blessing, J.J., Boersma, K.S., Bogan, M.T., Bonada, N., Bond, N.R., Bruder, A.,  
681 Burrows, R.M., Cancellario, T., Canhoto, C., Carlson, S.M., Cid, N., Danger, M.,  
682 Terra, B.D.F., Girolamo, A.M. De, Barra, E.D. La, Dyer, F., Elozegi, A., Faye, E.,  
683 Febria, C., Four, B., Gafny, S., Ghate, S.D., Guareschi, S., Hoppeler, F., Hwan,  
684 J.L., Jones, J.I., Kubheka, S., Laini, A., Langhans, S.D., Leigh, C., Little, C.J.,  
685 Lorenz, S., Marshall, J.C., Mcintosh, A.R., Meyer, E.I., Mlambo, M.C., Morais,  
686 M., Moya, N., Negus, P.M., Niyogi, D.K., Papatheodoulou, A., Pardo, I., Pauls,  
687 S.U., Robinson, C.T., Rolls, R.J., Shumilova, O., Sridhar, K.R., Steward, A.L.,  
688 Storey, R., Taleb, A., Uzan, A., Vorste, R. Vander, Waltham, N.J., Zak, D., Zarfl,  
689 C., Zoppini, A., 2018. A global analysis of terrestrial plant litter dynamics in non-  
690 perennial waterways. *Nat. Geosci.* 11, 497–503. [https://doi.org/10.1038/s41561-](https://doi.org/10.1038/s41561-018-0134-4)  
691 [018-0134-4](https://doi.org/10.1038/s41561-018-0134-4)

692 Dean, W., 1974. Determination of carbonate and organic matter in calcareous sediments  
693 and sedimentary rocks by loss on ignition; comparison with other methods. *J.*  
694 *Sediment. Res.* 44, 242–248. [https://doi.org/10.1306/74D729D2-2B21-11D7-](https://doi.org/10.1306/74D729D2-2B21-11D7-8648000102C1865D)  
695 [8648000102C1865D](https://doi.org/10.1306/74D729D2-2B21-11D7-8648000102C1865D)

696 DelSontro, T., Beaulieu, J.J., Downing, J.A., 2018. Greenhouse gas emissions from  
697 lakes and impoundments: Upscaling in the face of global change. *Limnol.*  
698 *Oceanogr. Lett.* 3, 64–75. <https://doi.org/10.1002/lol2.10073>

699 Deshmukh, C., Guérin, F., Vongkhamsoo, A., Pighini, S., Oudone, P., Sopraseuth, S.,

700 Godon, A., Rode, W., Guédant, P., Oliva, P., Audry, S., Zouiten, C., Galy-Lacaux,  
701 C., Robain, H., Ribolzi, O., Kansal, A., Chanudet, V., Descloux, S., Serça, D.,  
702 2018. Carbon dioxide emissions from the flat bottom and shallow Nam Theun 2  
703 Reservoir: Drawdown area as a neglected pathway to the atmosphere.  
704 Biogeosciences 15, 1775–1794. <https://doi.org/10.5194/bg-15-1775-2018>

705 Di Baldassarre, G., Wanders, N., AghaKouchak, A., Kuil, L., Rangelcroft, S.,  
706 Veldkamp, T.I.E., Garcia, M., van Oel, P.R., Breinl, K., Van Loon, A.F., 2018.  
707 Water shortages worsened by reservoir effects. Nat. Sustain. 1, 617–622.  
708 <https://doi.org/10.1038/s41893-018-0159-0>

709 Drake, T.W., Raymond, P.A., Spencer, R.G.M., 2018. Terrestrial carbon inputs to  
710 inland waters: A current synthesis of estimates and uncertainty. Limnol. Oceanogr.  
711 Lett. 3, 132–142. <https://doi.org/10.1002/lol2.10055>

712 FAO, 2020. Soil testing methods: Global Soil Doctors Programme-A farmer to farmer  
713 training programme., Soil testing methods manual.  
714 <https://doi.org/https://doi.org/10.4060/ca2796en>

715 Friedl, G., Wüest, A., 2002. Disrupting biogeochemical cycles – Consequences of  
716 damming. Aquat. Sci. 64, 55–65. [https://doi.org/10.1016/0025-326x\(91\)90729-c](https://doi.org/10.1016/0025-326x(91)90729-c)

717 Fromin, N., Pinay, G., Montuelle, B., Landais, D., Ourcival, J.M., Joffre, R., Lensi, R.,  
718 2010. Impact of seasonal sediment desiccation and rewetting on microbial  
719 processes involved in greenhouse gas emissions. Ecohydrology 3, 339–348.  
720 <https://doi.org/10.1002/eco.115>

721 Gallo, E.L., Lohse, K.A., Ferlin, C.M., Meixner, T., Brooks, P.D., 2014. Physical and  
722 biological controls on trace gas fluxes in semi-arid urban ephemeral waterways.  
723 Biogeochemistry 121, 189–207. <https://doi.org/10.1007/s10533-013-9927-0>

724 Gómez-Gener, L., Obrador, B., Marcé, R., Acuña, V., Catalán, N., Casas-Ruiz, J.P.,

725 Sabater, S., Muñoz, I., von Schiller, D., 2016. When Water Vanishes: Magnitude  
726 and Regulation of Carbon Dioxide Emissions from Dry Temporary Streams.  
727 *Ecosystems* 19, 710–723. <https://doi.org/10.1007/s10021-016-9963-4>

728 Gómez-gener, L., Obrador, B., Schiller, D. Von, Marcé, R., Casas-ruiz, P., Proia, L.,  
729 Acuña, V., Catalán, N., Muñoz, I., Koschorreck, M., 2015. Hot spots for carbon  
730 emissions from Mediterranean fluvial networks during summer drought.  
731 *Biogeochemistry* 125, 409–426. <https://doi.org/10.1007/s10533-015-0139-7>

732 Granéli, W., Lindell, M., Tranvik, L., 1996. Photo-oxidative production of dissolved  
733 inorganic carbon in lakes of different humic content. *Limnol. Oceanogr.* 41, 698–  
734 706. <https://doi.org/10.4319/lo.1996.41.4.0698>

735 Grasset, C., Mendonça, R., Villamor Saucedo, G., Bastviken, D., Roland, F., Sobek, S.,  
736 2018. Large but variable methane production in anoxic freshwater sediment upon  
737 addition of allochthonous and autochthonous organic matter. *Limnol. Oceanogr.*  
738 63, 1488–1501. <https://doi.org/10.1002/lno.10786>

739 Halekoh, U., Højsgaard, S., 2014. A kenward-Roger approximation and parametric  
740 bootstrap methods for tests in linear mixed models-the R package pbkrtest. *J. Stat.*  
741 *Softw.* 59, 1–32. <https://doi.org/10.18637/jss.v059.i09>

742 Harrison, J.A., Deemer, B.R., Birchfield, M.K., O'Malley, M.T., 2017. Reservoir  
743 Water-Level Drawdowns Accelerate and Amplify Methane Emission. *Environ.*  
744 *Sci. Technol.* 51, 1267–1277. <https://doi.org/10.1021/acs.est.6b03185>

745 Heathcote, A.J., Anderson, N.J., Prairie, Y.T., Engstrom, D.R., Del Giorgio, P.A., 2015.  
746 Large increases in carbon burial in northern lakes during the Anthropocene. *Nat.*  
747 *Commun.* 6, 1–6. <https://doi.org/10.1038/ncomms10016>

748 Heilman, M.A., Carlton, R.G., 2001. Methane oxidation associated with submersed  
749 vascular macrophytes and its impact on plant diffusive methane flux.

750 Biogeochemistry 52, 207–224. <https://doi.org/10.1023/A:1006427712846>

751 Jäckel, U., Schnell, S., Conrad, R., 2001. Effect of moisture, texture and aggregate size  
752 of paddy soil on production and consumption of CH<sub>4</sub>. Soil Biol. Biochem. 33,  
753 965–971. [https://doi.org/10.1016/S0038-0717\(00\)00248-0](https://doi.org/10.1016/S0038-0717(00)00248-0)

754 Jin, H., Yoon, T.K., Lee, S.-H., Kang, H., Im, J., Park, J.-H., 2016. Enhanced  
755 greenhouse gas emission from exposed sediments along a hydroelectric reservoir  
756 during an extreme drought event. Environ. Res. Lett. 11, 1–10.  
757 <https://doi.org/10.1088/1748-9326/11/12/124003>

758 Keller, P.S., Catalán, N., Schiller, D. von, Grossart, H.-P., Koschorreck, M., Obrador,  
759 B., Frassl, M.A., Karakaya, N., Barros, N., Howitt, J.A., Mendoza-Lera, C., Pastor,  
760 A., Flaim, G., Aben, R., Riis, T., Arce, M.I., Onandia, G., Paranaíba, J.R.,  
761 Linkhorst, A., Campo, R. del, Amado, A.M., Cauvy-Fraunié, S., Brothers, S.,  
762 Condon, J., Mendonça, R.F., Reverey, F., Rõõm, E.-I., Datry, T., Roland, F., Laas,  
763 A., Obertegger, U., Park, J.-H., Wang, H., Kosten, S., Gómez, R., Feijoó, C.,  
764 Elosegí, A., Sánchez-Montoya, M.M., Finlayson, C.M., Melita, M., Junior, E.S.O.,  
765 Muniz, C.C., Gómez-Gener, L., Leigh, C., Zhang, Q., Marcé, R., 2020. Global  
766 CO<sub>2</sub> emissions from dry inland waters share common drivers across ecosystems.  
767 Nat. Commun. 11, 1–8. <https://doi.org/10.1038/s41467-020-15929-y>

768 Keller, P.S., Marcé, R., Obrador, B., Koschorreck, M., 2021. Global carbon budget of  
769 reservoirs is overturned by the quantification of drawdown areas. Nat. Geosci. 1–  
770 19. <https://doi.org/10.1038/s41561-021-00734-z>

771 Kemenes, A., Forsberg, B.R., Melack, J.M., 2016. Downstream emissions of CH<sub>4</sub> and  
772 CO<sub>2</sub> from hydroelectric reservoirs (Tucuruí, Samuel, and Curua-Una) in the  
773 Amazon basin. Inl. Waters 6, 295–302. <https://doi.org/10.5268/IW-6.3.980>

774 Kenward, M.G., Roger, J.H., 1997. Small Sample Inference for Fixed Effects from

775       Restricted Maximum Likelihood. *Biometrics* 53, 983.  
776       <https://doi.org/10.2307/2533558>

777   Koschorreck, M., 2000. Methane turnover in exposed sediments of an Amazon  
778       floodplain lake. *Biogeochemistry* 50, 195–206.  
779       <https://doi.org/10.1023/A:1006326018597>

780   Koschorreck, M., Darwich, A., 2003. Nitrogen dynamics in seasonally flooded soils in  
781       the Amazon floodplain. *Wetl. Ecol. Manag.* 11, 317–330.

782   Kosten, S., van den Berg, S., Mendonça, R., Paranaíba, J.R., Roland, F., Sobek, S., Van  
783       Den Hoek, J., Barros, N., 2018. Extreme drought boosts CO<sub>2</sub> and CH<sub>4</sub> emissions  
784       from reservoir drawdown areas. *Inl. Waters* 8, 329–340.  
785       <https://doi.org/10.1080/20442041.2018.1483126>

786   Kottek, M., Grieser, J., Beck, C., Rudolf, B., Rubel, F., 2006. World Map of the  
787       Köppen-Geiger climate classification updated. *Meteorol. Zeitschrift* 15, 259–263.  
788       <https://doi.org/10.1127/0941-2948/2006/0130>

789   Kuznetsova, A., Brockhoff, P.B., Christensen, R.H.B., 2017. lmerTest Package: Tests in  
790       Linear Mixed Effects Models. *J. Stat. Softw.* 82, 1–26.  
791       <https://doi.org/10.18637/jss.v082.i13>

792   Leigh, C., Boulton, A.J., Courtwright, J.L., Fritz, K., May, C.L., Walker, R.H., Datry,  
793       T., 2016. Ecological research and management of intermittent rivers: an historical  
794       review and future directions. *Freshw. Biol.* 61, 1181–1199.  
795       <https://doi.org/10.1111/fwb.12646>

796   Lesmeister, L., Koschorreck, M., 2017. A closed-chamber method to measure  
797       greenhouse gas fluxes from dry aquatic sediments. *Atmos. Meas. Tech.* 10, 2377–  
798       2382. <https://doi.org/10.5194/amt-10-2377-2017>

799   Lischeid, G., Kalettka, T., 2012. Grasping the heterogeneity of kettle hole water quality

800 in Northeast Germany. *Hydrobiologia* 689, 63–77. <https://doi.org/10.1007/s10750->  
801 011-0764-7

802 Lo, S., Andrews, S., 2015. To transform or not to transform: using generalized linear  
803 mixed models to analyse reaction time data. *Front. Psychol.* 6, 1–16.  
804 <https://doi.org/10.3389/fpsyg.2015.01171>

805 Manzoni, S., Schimel, J.P., Porporato, A., 2012. Responses of soil microbial  
806 communities to water stress : results from a meta-analysis. *Ecology* 93, 930–938.  
807 <https://doi.org/10.1890/11-0026.1>

808 Marcé, R., Obrador, B., Gómez-Gener, L., Catalán, N., Koschorreck, M., Arce, M.I.,  
809 Singer, G., von Schiller, D., 2019. Emissions from dry inland waters are a blind  
810 spot in the global carbon cycle. *Earth-Science Rev.* 188, 240–248.  
811 <https://doi.org/10.1016/j.earscirev.2018.11.012>

812 Mattson, M.D., Likens, G.E., 1992. Redox reactions of organic matter decomposition in  
813 a soft water lake. *Biogeochemistry* 19, 149–172.  
814 <https://doi.org/10.1007/BF00000876>

815 Mendonça, R., Müller, R.A., Clow, D., Verpoorter, C., Raymond, P., Tranvik, L.J.,  
816 Sobek, S., 2017. Organic carbon burial in global lakes and reservoirs. *Nat.*  
817 *Commun.* 8, 1–6. <https://doi.org/10.1038/s41467-017-01789-6>

818 Messenger, M.L., Lehner, B., Cockburn, C., Lamouroux, N., Pella, H., Snelder, T.,  
819 Tockner, K., Trautmann, T., Watt, C., Datry, T., 2021. Global prevalence of non-  
820 perennial rivers and streams. *Nature* 594, 391–397. <https://doi.org/10.1038/s41586->  
821 021-03565-5

822 Myhre, G., Shindell, D., Bréon, F.-M., Collins, W., Fuglestvedt, J., Huang, J., Koch, D.,  
823 Lamarque, J.-F., Lee, D., Mendoza, B., Nakajima, T., Robock, A., Stephens, G.,  
824 Takemura, T., Zhang, H., Stocker, T.F., Qin, D., Plattner, G.-K., Tignor, M., Allen,

825 S.K., Doschung, J., Nauels, A., Xia, Y., Bex, V., Midgley, P.M., 2013.  
826 Anthropogenic and natural radiative forcing. In *Climate Change 2013: The*  
827 *Physical Science Basis. Contribution of Working Group I to the Fifth Assessment*  
828 *Report of the Intergovernmental Panel on Climate Change. Cambridge University*  
829 *Press, pp. 659–740. <https://doi.org/10.1017/CBO9781107415324.018>.*

830 Naimi, B., Hamm, N.A.S., Groen, T.A., Skidmore, A.K., Toxopeus, A.G., 2014. Where  
831 is positional uncertainty a problem for species distribution modelling? *Ecography*  
832 *(Cop.)*. 37, 191–203. <https://doi.org/10.1111/j.1600-0587.2013.00205.x>

833 Obrador, B., Von Schiller, D., Marcé, R., Gómez-Gener, L., Koschorreck, M., Borrego,  
834 C., Catalán, N., 2018. Dry habitats sustain high CO<sub>2</sub> emissions from temporary  
835 ponds across seasons. *Sci. Rep.* 8, 1–12. [https://doi.org/10.1038/s41598-018-](https://doi.org/10.1038/s41598-018-20969-y)  
836 [20969-y](https://doi.org/10.1038/s41598-018-20969-y)

837 Onandia, G., Maassen, S., Musseau, C.L., Berger, S.A., Olmo, C., Jeschke, J.M.,  
838 Lischeid, G., 2021. Key drivers structuring rotifer communities in ponds: Insights  
839 into an agricultural landscape. *J. Plankton Res.* 43, 396–412.  
840 <https://doi.org/10.1093/plankt/fbab033>

841 Paranaíba, J.R., Quadra, G., Josué, I.I.P., Almeida, R.M., Mendonça, R., Cardoso, S.J.,  
842 Silva, J., Kosten, S., Campos, J.M., Almeida, J., Araújo, R.L., Roland, F., Barros,  
843 N., 2020. Sediment drying-rewetting cycles enhance greenhouse gas emissions,  
844 nutrient and trace element release, and promote water cytogenotoxicity. *PLoS One*  
845 15, 1–21. <https://doi.org/10.1371/journal.pone.0231082>

846 Pekel, J., Cottam, A., Gorelick, N., Belward, A.S., 2016. High-resolution mapping of  
847 global surface water and its long-term changes. *Nature* 540, 418–422.  
848 <https://doi.org/10.1038/nature20584>

849 R Core Team, 2018. R: A language and environment for statistical computing.

850 Raymond, P.A., Hartmann, J., Lauerwald, R., Sobek, S., McDonald, C., Hoover, M.,  
851 Butman, D., Striegl, R., Mayorga, E., Humborg, C., Kortelainen, P., Dürr, H.,  
852 Meybeck, M., Ciais, P., Guth, P., 2013. Global carbon dioxide emissions from  
853 inland waters. *Nature* 503, 355–359. <https://doi.org/10.1038/nature12760>

854 Rodrigo, A., Recous, S., Neel, C., Mary, B., 1997. Modelling temperature and moisture  
855 effects on C-N transformations in soils: Comparison of nine models. *Ecol. Modell.*  
856 102, 325–339. [https://doi.org/10.1016/S0304-3800\(97\)00067-7](https://doi.org/10.1016/S0304-3800(97)00067-7)

857 Rosentreter, J.A., Borges, A. V., Deemer, B.R., Holgerson, M.A., Liu, S., Song, C.,  
858 Melack, J., Raymond, P.A., Duarte, C.M., Allen, G.H., Olefeldt, D., Poulter, B.,  
859 Battin, T.I., Eyre, B.D., 2021. Half of global methane emissions come from highly  
860 variable aquatic ecosystem sources. *Nat. Geosci.* 14, 225–234.  
861 <https://doi.org/https://doi.org/10.1038/s41561-021-00715-2>

862 Serça, D., Deshmukh, C., Pighini, S., Oudone, P., Vongkhamsoo, A., Guédant, P., Rode,  
863 W., Godon, A., Chanudet, V., Descloux, S., Guérin, F., 2016. Nam Theun 2  
864 Reservoir four years after commissioning: significance of drawdown methane  
865 emissions and other pathways. *Hydroécologie Appliquée* 19, 119–146.  
866 <https://doi.org/10.1051/hydro/2016001>

867 Serrano-Silva, N., Sarria-Guzmán, Y., Dendooven, L., Luna-Guido, M., 2014.  
868 Methanogenesis and Methanotrophy in Soil : A Review. *Pedosphere* 24, 291–307.  
869 [https://doi.org/10.1016/S1002-0160\(14\)60016-3](https://doi.org/10.1016/S1002-0160(14)60016-3)

870 Sobek, S., Delsontro, T., Wongfun, N., Wehrli, B., 2012. Extreme organic carbon burial  
871 fuels intense methane bubbling in a temperate reservoir. *Geophys. Res. Lett.* 39, 2–  
872 5. <https://doi.org/10.1029/2011GL050144>

873 Sponseller, R.A., 2007. Precipitation pulses and soil CO<sub>2</sub> flux in a Sonoran Desert  
874 ecosystem. *Glob. Chang. Biol.* 13, 426–436. <https://doi.org/10.1111/j.1365->

875 2486.2006.01307.x

876 Steward, A.L., Schiller, D. Von, Tockner, K., Marshall, J.C., Bunn, S.E., Steward, A.L.,  
877 Schiller, D. Von, Tockner, K., Marshall, J.C., Bunn, S.E., 2012. When the river  
878 runs dry : human and ecological values of dry riverbeds. *Front. Ecol. Environ.* 10,  
879 202–209. <https://doi.org/10.1890/110136>

880 Strom, L., Ekberg, A., Mastepanov, M., Christensen, T.R., 2003. The effect of vascular  
881 plants on carbon turnover and methane emissions from a tundra wetland. *Glob.*  
882 *Chang. Biol.* 9, 1185–1192. [https://doi.org/https://doi.org/10.1046/j.1365-](https://doi.org/https://doi.org/10.1046/j.1365-2486.2003.00655.x)  
883 [2486.2003.00655.x](https://doi.org/https://doi.org/10.1046/j.1365-2486.2003.00655.x)

884 Tranvik, L.J., Downing, J.A., Cotner, J.B., Loiselle, S.A., Striegl, R.G., Ballatore, T.J.,  
885 Dillon, P., Finlay, K., Fortino, K., Knoll, L.B., Kortelainen, P.L., Kutser, T.,  
886 Larsen, S., Laurion, I., Leech, D.M., Leigh McCallister, S., McKnight, D.M.,  
887 Melack, J.M., Overholt, E., Porter, J.A., Prairie, Y., Renwick, W.H., Roland, F.,  
888 Sherman, B.S., Schindler, D.W., Sobek, S., Tremblay, A., Vanni, M.J., Verschoor,  
889 A.M., Von Wachenfeldt, E., Weyhenmeyer, G.A., 2009. Lakes and reservoirs as  
890 regulators of carbon cycling and climate. *Limnol. Oceanogr.* 54, 2298–2314.  
891 [https://doi.org/10.4319/lo.2009.54.6\\_part\\_2.2298](https://doi.org/10.4319/lo.2009.54.6_part_2.2298)

892 Van Cappellen, P., Maavara, T., 2016. Rivers in the Anthropocene: Global scale  
893 modifications of riverine nutrient fluxes by damming. *Ecohydrol. Hydrobiol.* 16,  
894 106–111. <https://doi.org/10.1016/j.ecohyd.2016.04.001>

895 von Fischer, J.C., Hedin, L.O., 2007. Controls on soil methane fluxes: Tests of  
896 biophysical mechanisms using table isotope tracers. *Global Biogeochem. Cycles*  
897 21, 1–9. <https://doi.org/10.1029/2006GB002687>

898 von Schiller, D., Marcé, R., Obrador, B., Gómez-Gener, L., Casas-Ruiz, J.P., Acuña, V.,  
899 Koschorreck, M., 2014. Carbon dioxide emissions from dry watercourses. *Inl.*

900 Waters 4, 377–382. <https://doi.org/10.5268/IW-4.4.746>

901 Welles, J.M., Demetriades-Shah, T.H., McDermitt, D.K., 2001. Considerations for  
902 measuring ground CO<sub>2</sub> effluxes with chambers. *Chem. Geol.* 177, 3–13.  
903 [https://doi.org/10.1016/S0009-2541\(00\)00388-0](https://doi.org/10.1016/S0009-2541(00)00388-0)

904 Wurtsbaugh, W.A., Miller, C., Null, S.E., Justin De Rose, R., Wilcock, P.,  
905 Hahnenberger, M., Howe, F., Moore, J., 2017. Decline of the world’s saline lakes.  
906 *Nat. Geosci.* 10, 816–821. <https://doi.org/10.1038/NGEO3052>

907 Yvon-Durocher, G., Allen, A.P., Bastviken, D., Conrad, R., Gudasz, C., St-Pierre, A.,  
908 Thanh-Duc, N., Del Giorgio, P.A., 2014. Methane fluxes show consistent  
909 temperature dependence across microbial to ecosystem scales. *Nature* 507, 488–  
910 491. <https://doi.org/10.1038/nature13164>

911

System type	CH <sub>4</sub> flux (mg CH <sub>4</sub> m <sup>-2</sup> d <sup>-1</sup> )	Reference
<b>Lakes (n = 45)</b>		
<i>Dry sediment</i>	48 ± 91	
<i>Uphill soil</i>	1 ± 5	
<b>Ponds (n = 16)</b>		
<i>Dry sediment</i>	38 ± 63	
<i>Uphill soil</i>	0.3 ± 1	
<b>Reservoirs (n = 19)</b>		
<i>Dry sediment</i>	36 ± 78	This study
<i>Uphill soil</i>	2 ± 4	
<b>Streams (n = 9)</b>		
<i>Dry sediment</i>	7 ± 17	
<i>Uphill soil</i>	0.2 ± 0.7	
<b>All systems (n = 89)</b>		
<i>Dry sediment</i>	40 ± 80	
<i>Uphill soil</i>	1 ± 4	
<b>Lake (Brazil)</b>	1.4 ± 0.15 ( <i>Amazonian floodplain</i> )	Koschorreck, 2000
<b>Ponds (Spain)</b>	4.8 ± 3.8 ( <i>Dry bed</i> )	Obrador et al. 2018
<b>Reservoir (Brazil)</b>	0.9 ± 6.9 ( <i>Drawdown</i> )	Amorim et al. 2019
<b>Reservoir (China)</b>	7 ± 8.9 ( <i>Drawdown</i> )	Chen et al. 2011
<b>Reservoir (China)</b>	4 ± 1.5 ( <i>Drawdown</i> )	Yang et al. 2012
<b>Reservoir (China)</b>	7.7 ± 5 ( <i>Drawdown</i> )	Hao et al. 2019
<b>Reservoir (Laos)</b>	27 ± 36 ( <i>Drawdown</i> )	Serça et al. 2016
<b>Reservoir (Germany)</b>	4.1 <sup>a</sup> ( <i>Drawdown</i> )	Marcé et al. 2019
<b>Reservoir (Germany)</b>	7.2 <sup>a</sup> ( <i>Drawdown</i> )	Marcé et al. 2019
<b>Reservoir (Spain)</b>	0 ( <i>Drawdown</i> )	Marcé et al. 2019
<b>Reservoir (Spain)</b>	4.1 <sup>a</sup> ( <i>Drawdown</i> )	Marcé et al. 2019
<b>Reservoir (Spain)</b>	0.3 <sup>a</sup> ( <i>Drawdown</i> )	Marcé et al. 2019
<b>Streams (United States)</b>	0.4 ± 0.5 ( <i>Dry river bed</i> )	Gallo et al. 2014
<b>Streams (Spain)</b>	3.2 ± 0.9 ( <i>Dry river and impoundment beds</i> )	Gómez-Gener et al. 2015
<b>Global CH<sub>4</sub> flux rates from surface waters (mg CH<sub>4</sub> m<sup>-2</sup> d<sup>-1</sup>)</b>		
<b>Lakes</b>	153 ± 293	Rosentreter et al. 2021
<b>Ponds</b>	12 ± 30	Holgerson and Raymond 2016
<b>Reservoirs</b>	165 ± 369	Rosentreter et al. 2021
<b>Streams</b>	112 ± 425	Rosentreter et al. 2021

<sup>a</sup> Mean values

Input variable	CH <sub>4</sub> flux			
	$\beta$	<i>SE</i>	<i>t-value</i>	<i>CI</i>
<b>(Intercept)</b>	3.53	0.30	11.64	2.93 – 4.12
<b>Interaction (Organic matter:Sediment temperature)</b>	0.39	0.10	3.69	0.18 – 0.59
<b>Organic matter</b>	-0.54	0.15	-3.55	-0.85 – -0.24
<b>Moisture</b>	0.49	0.15	3.20	0.19 – 0.79
<b>Conductivity</b>	0.37	0.12	3.01	0.12 – 0.61
<b>Elevation</b>	0.35	0.17	1.98	0.004 – 0.7
<b>Interaction (Moisture:Organic matter)</b>	-0.20	0.10	-2.01	-0.41 – -0.006
<b>R<sup>2</sup>m</b>	0.23			
<b>R<sup>2</sup>c</b>	0.57			

<b>System type</b>	<b>Area of exposed aquatic sediments during one year <sup>a</sup></b>	<b>CH<sub>4</sub> emission rate</b>	<b>Cross-continental CH<sub>4</sub> emission</b>	<b>Cross-continental CH<sub>4</sub> emission in CO<sub>2</sub> equivalents</b>	<b>Cross-continental CH<sub>4</sub> emission as C emission</b>
	<b>(km<sup>2</sup>)</b>	<b>(mg CH<sub>4</sub> m<sup>-2</sup> d<sup>-1</sup>)</b>	<b>(Tg CH<sub>4</sub> y<sup>-1</sup>)</b>	<b>(Pg CO<sub>2</sub>-eq y<sup>-1</sup>)</b>	<b>(Tg C y<sup>-1</sup>)</b>
<b>Lakes and reservoirs</b>	187,542 (Marcé et al., 2019)	44 ± 10.9	3.1 ± 0.7	0.1 ± 0.02	2.3 ± 0.5
<b>Ponds</b>	18,390 (Marcé et al., 2019)	38 ± 15.7	0.26 ± 0.1	0.009 ± 0.003	0.2 ± 0.08
<b>Streams and rivers</b>	84,461 (Raymond et al., 2013)	7 ± 5.6	0.21 ± 0.1	0.007 ± 0.006	0.16 ± 0.13
<b>Total</b>	290,393		3.6 ± 0.4	0.11 ± 0.01	2.7 ± 0.3

<sup>a</sup> *Seasonal and permanent exposure*

Figure 1

[Click here to access/download;Figure;Fig1.tif](#)

